GEOLOGICA BELGICA
2026, Vol. 29/1-2, 37–64
https://doi.org/10.20341/gb.2026.003

A study of the early Oligocene and early Miocene *Diplocynodon* (Crocodylia) material housed in the Filhol collection of KU Leuven (Belgium)

Anne BASTEN

Earth and Environmental Sciences, KU Leuven, Celestijnenlaan 200E, 3001 Leuven, Belgium; corresponding author: bastenae@gmail.com.

Pascal VAN DER BIJ

Earth and Environmental Sciences, KU Leuven, Celestijnenlaan 200E, 3001 Leuven, Belgium.

Wouter BERINGS

Earth and Environmental Sciences, KU Leuven, Celestijnenlaan 200E, 3001 Leuven, Belgium.

Sophie A. C. M. BOERMAN

Earth and Environmental Sciences, KU Leuven, Celestijnenlaan 200E, 3001 Leuven, Belgium; OD Earth and History of Life, Institute of Natural Sciences, Vautierstraat 29, 1000 Brussels, Belgium.

Johan VELLEKOOP

Earth and Environmental Sciences, KU Leuven, Celestijnenlaan 200E, 3001 Leuven, Belgium; OD Earth and History of Life, Institute of Natural Sciences, Vautierstraat 29, 1000 Brussels, Belgium.

ABSTRACT

Diplocynodon is an enigmatic extinct genus that is generally considered to be part of the Alligatoroidea, Crocodylia. While Alligatoroidea potentially originated in North America, *Diplocynodon* only has a fossil record in Europe, dating from the middle Eocene to middle Miocene (c. 45–15 Ma). The study of *Diplocynodon* remains curated in palaeontological collections could aid research on the morphology, phylogeny, evolution and biogeography of this large and widespread genus. We describe the *Diplocynodon* material in the historical Filhol collection of KU Leuven, collected at Saint-Gérand-le-Puy (early Miocene) and Ronzon (early Oligocene), from central France in the late 19th century. The aim was to identify which remains reside in the Filhol collection and to deduce the systematics behind these remains, making the collection more accessible to future research. A total of 781 skeletal elements were catalogued, including both cranial and postcranial bones. The most complete and anatomically representative specimens were photographed. Based on characteristic features, the remains from Saint-Gérand-le-Puy were confirmed as *D. ratelii*, a taxon that has previously been described from that locality. The remains from Ronzon could not be confidently determined in the present study.

KEYWORDS

palaeontology,
Eusuchia,
systematics,
historical collections

Article history
Received 01.09.2025, accepted in revised form 09.03.2026, available online 27.08.2026.

1. Introduction

Crown-group Crocodylia are a group of archosaurs comprising around 140 species (both extant and extinct species), with their origins firmly dating back to the Cretaceous period (Roos et al., 2007; Oaks, 2011; Turner et al., 2017; Lee & Yates, 2018; Pan et al., 2021; Rio & Mannion, 2021; Darlim et al., 2022). They encompass several taxonomic groups, primarily crocodiles (Crocodylidae), gharials (Gavialidae; comprising the extant taxa *Gavialis* and *Tomistoma*) and alligators (Alligatoridae). Until as recently as the Neogene (c. 23–2.5 Ma), Europe hosted all three major clades of crown-group Crocodylia (Delfino et al., 2007; Prista et al., 2015). Crocodylidae, represented by *Crocodylus*, dates back to 5–6 Ma (Delfino et al., 2007). Gavialidae was represented by *Gavialosuchus* and/or *Tomistoma*, which became extinct in Europe around 10 Ma, while Alligatoroidea potentially included the enigmatic genus *Diplocynodon*, which went extinct approximately 13.5 Ma, with disputed remains reported until 6.2 Ma (Delfino et al., 2007; Rio & Mannion, 2021).

Alligatoroidea originated in the Late Cretaceous (Lee & Yates, 2018; Darlim et al., 2022), and *Diplocynodon* is generally perceived as one of the most basally branching lineages within this group (Brochu, 1999; Martin et al., 2014; Rio et al., 2020). However, the phylogenetic relationships within the genus *Diplocynodon* remain largely inconsistent across studies, sometimes being classified as paraphyletic with various clades branching off at different times (Delfino & Smith, 2012; Martin et al., 2014; Macaluso et al., 2019; Rio & Mannion, 2021; Massonne & Böhme, 2022; Venczel & Codrea, 2022). *Diplocynodon* could appear monophyletic due to the loss of apomorphies or independent evolutionary developments within other alligatoroids (Rio & Mannion, 2021). Alternatively, *Diplocynodon* has been recovered as a monophyletic stem-group crocodylian in one clade with *Borealosuchus* (Walter et al., 2025). As of 2025, 14 species of *Diplocynodon* are recognized in the literature, but not all of them as valid (Table 1).

Extant Alligatoridae includes two subfamilies, Alligatorinae and Caimaninae, encompassing a total of eight species distributed across North and South America, except for *Alligator sinensis* found in Asia (Martin, S., 2007). The origin of the Alligatoridae is suggested to be in North America (Groh et al., 2023). Yet, *Diplocynodon* is solely documented in Europe, and its dispersal to the continent remains ambiguous (Martin et al., 2014; Massonne & Böhme, 2022). A European origin has been proposed, but the absence of early branching Paleogene alligatoroids in Europe leaves this hypothesis uncertain (Puértolas-Pascual et al., 2016; Groh et al., 2023). This gap in the fossil record instead suggests a possible post-extinction immigration from North America or Asia (Martin et al., 2014; Puértolas-Pascual et al., 2016). Speculations about a North American origin stem from its supposed close phylogenetic relationship with the North American genus *Leidyosuchus* (Martin et al., 2014; Rio & Mannion, 2021) or *Borealosuchus* (Walter et al., 2025). A novel phylogeny which places *Diplocynodon* together with *Borealosuchus* outside of Crocodylia offers a potential explanation for the extended gap in the European record and supports a North American origin (Walter et al., 2025). Some authors even suggest a Central Asian origin due to an initial appraisal of similarities with still undescribed material (Kuzmin & Zvonok, 2021).

Despite multiple analyses attempting to diagnose and classify *Diplocynodon*, the diagnostic characteristics are highly variable and complex, and the synapomorphies identified in previous

Table 1. All 14 currently described *Diplocynodon* species.

Name	Age	Source material	Location	First description (from source material)
**D. "buetikonensis"*	Miocene	Scheyer et al., 2015	Switzerland	von Meyer, 1854
D. darwini	middle Eocene	Hastings & Hellmund, 2015	Germany	Ludwig, 1877
D. deponiae	middle Eocene	Delfino & Smith, 2012	Germany	Frey et al., 1987
D. elavericus	late Eocene	Martin, 2010	France	Martin, 2010
**D. "gervaisi"*	early Oligocene	Berg, 1966	France	Gervais, 1859
D. hantoniensis	late Eocene	Rio et al., 2020	United Kingdom	Wood, 1846
⁺D. "kintyktshensis"	early/middle Miocene	Skučas et al., 2015	Kazakhstan	Efimov, 1988
D. kochi	late Eocene	Venczel & Codrea, 2022	Romania	Venczel & Codrea, 2022
D. levantinicum	late Oligocene	Massonne & Böhme, 2022	Bulgaria	Huene & Nikoloff, 1963
D. muelleri	early Oligocene	Piras & Buscalioni, 2006	Spain	Kälin, 1936
D. ratelii	early Miocene	Díaz Aráez et al., 2017	France, Spain	Pomel, 1847
D. remensis	late Paleocene	Martin et al., 2014	France	Martin et al., 2014
D. tormis	middle Eocene	Serrano-Martínez et al., 2019	Spain	Buscalioni et al., 1992
D. ungeri	middle Miocene	Martin & Gross, 2011	Austria	Prangner, 1845

*Currently not accepted because of poor preservation or a need for revision (Massonne & Böhme, 2022).

⁺Currently not accepted due to lack of description or diagnostic criteria (Skučas et al., 2015).

studies have not been consistently supported, further complicating species identification and taxonomic assessments (Brochu, 1999; Rio et al., 2020; Rio & Mannion, 2021). However, a recent revision of the genus by Walter et al. (2026) has substantially improved our understanding of diagnostic characters among the different species of *Diplocynodon*.

The distribution of modern crocodylians is mainly restricted by temperature (mean annual >14.2 °C; Markwick, 1998) and saltwater tolerance (Brochu, 1999; Górka et al., 2025), and standing water is an essential buffer against temperature extremes. Climate reconstructions indicate that warm and humid conditions prevailed in Europe throughout the Paleogene and Neogene (Mosbrugger et al., 2005; Westerhold et al., 2020), consistent with the presence of *Diplocynodon* during this interval. Such an environment is e.g. present in fluvio-lacustrine systems with flooding forests in close proximity, which have both aquatic and terrestrial parts in the landscape (Luján et al., 2019; Górka et al., 2025). Indeed, warm and humid environments have been recorded in the Paleogene and Neogene in different places throughout Europe, ranging from the Iberian Peninsula to the Czech Republic and the Transylvanian Basin (Díaz Aráez et al., 2017; Luján et al., 2019; Venczel, 2023), often concurring with occurrences of *Diplocynodon*.

The study of *Diplocynodon* remains curated in historical palaeontological collections could aid research on the morphology, phylogeny, evolution and biogeography of this genus. This study therefore focuses on the crocodylian remains in the historical Filhol collection of KU Leuven, comprising abundant *Diplocynodon* material. The Filhol collection holds an abundance of vertebrate remains from several Paleogene–Neogene localities and regions in central and southern France, in particular from the Quercy region (the "Phosphorites du Quercy"), Saint-Gérand-le-Puy and Ronzon (Filhol, 1876/1877, 1879/1880, 1881). The fossils housed in this collection were originally collected and studied at the end of the 19th century by Henri Filhol, a renowned French physician, geologist, palaeontologist and natural historian (Filhol, 1876/1877, 1879/1880, 1881; Anonymous, 1902). The collection was subsequently acquired by KU Leuven professor, Henry de Dorlodot, in the early 20th century. The Filhol collection predominantly consists of mammalian material, including several holotypes and paratypes (e.g. *Amphicyon ambiguus*; KU Leuven PLV544; Filhol, 1876/1877; *Pseudocyonopsis antiquus primigenius*; KU Leuven PLV1507; Springhorn, 1977), but it also includes other groups, such as birds and crocodiles. Most of the specimens are sorted according to order or class and contain further information about taxonomy, classification and provenance. The specimens are generally disarticulated and removed from their sedimentary matrix. Despite previous studies (e.g. Filhol, 1883; Teilhard de Chardin, 1915; Springhorn, 1977; Lange-Badré, 1979; Fournier et al., 2020; Solé et al., 2021), a large part of this collection remains insufficiently described. For example, while Filhol conducted extensive work on the mammal material from Saint-Gérand-le-Puy and Ronzon (Filhol 1876/1877, 1879/1880, 1881; Anonymous, 1902), the Crocodylia from this collection have not been studied so thoroughly. The material from Saint-Gérand-le-Puy and Ronzon comprises a variety of crocodylian remains ascribed to *Diplocynodon*, likely determined by Henri Filhol himself as he studied material from both and ascribed material to *Diplocynodon* from other localities (Filhol 1876/1877, 1879/1880, 1881). The *Diplocynodon* material from Saint-Gérand-le-Puy consists of disarticulated cranial and postcranial bones, generally yellow-brown in colour, occasionally with coarse sandy matrix material attached, collectively catalogued under KU Leuven PLV1983. The material from Ronzon, consisting of partially articulated cranial and postcranial bones in several blocks of greyish marly limestone, has remained uncatalogued.

The aim of this study is to systematically describe the fossil remains of Crocodylia housed in the Filhol collection, and ascertain their taxonomy and diversity, aiding the research on the enigmatic genus *Diplocynodon*. Through a comprehensive documentation of all remains found in this collection and a comparison to previously described specimens in literature, the research aims to disclose the number and type of remains present in the collection as well as the species to which they belong. This study and future research can improve the understanding of the environment and species composition at both localities. By documenting and analysing these specimens, this research aims to enhance our understanding of the morphological diversity and taxonomic composition of crocodylians represented in the Filhol collection. Preserving and cataloguing these fossils will ensure their availability for future scientific inquiry.

2. Material and methods

2.1. Localities

The stratigraphic successions of Saint-Gérand-le-Puy (Fig. 1) in the Limagne basin of central France, date back to the early Miocene and are significant for the many fossils recovered from fluvio-lacustrine calcareous and marly sediments (Pomel, 1847; Gervais, 1859; Filhol, 1883; Bucher et al., 1985). All work from Filhol was focused on specimens from a single well-defined horizon (Filhol, 1883), a green marl layer with aquatic and terrestrial vertebrates (Bucher et al., 1985), likely formed by a mud stream filling the area between already standing calcareous columns (Bucher et al., 1985). In reference to the paper of Bucher et al. (1985), Wattinne et al. (2003) also mentioned vertebrate fossils from a second layer, a calcareous sand layer. Nevertheless, Bucher et al. (1985) only mentions the green marls, where *Diplocynodon ratelii* was first recovered and described in the 1840s, from a quarry in Montaigu-le-Blin, in the surroundings of Saint-Gérand-le-Puy (Pomel, 1847). The limestone in the area of Saint-Gérand-le-Puy was known as "Calcaire à Phryganes" or as "Indusial Limestone" (Filhol, 1879/1880; Göhlich & Mourer-Chauviré, 2005).

In palaeontological literature, not only the quarry in Montaigu-le-Blin is often called Saint-Gérand-le-Puy, but deposits from Bransat, Chavroches, Langy, Poncenat, Cluzel, Billy and Saulcet are also sometimes referred to as Saint-Gérand-le-Puy (Cheneval, 1989; Göhlich & Mourer-Chauviré, 2005). All localities are the same age, calibrated to Mammal Neogene zone 2a (MN2a; late Aquitanian; Fig. 1) except Saulcet and Billy, which are calibrated to MN1 (early Aquitanian) and Bransat, for which the mammal zonation is unknown (Göhlich & Mourer-Chauviré, 2005). While MN2 is currently no longer split into subzones, because of the diachronic nature of the previously established MN2a/MN2b boundary (Mein, 1999), here we follow Mennecart et al. (2016), still applying the formerly used subzone MN2a (Montaigu), representing the lower part of MN2, since it is more specific in age.

Ronzon (Fig. 1), located 1.4 km southwest of Le Puy-en-Velay (southern France), is notable for its early Oligocene deposits, calibrated to Mammal Paleogene Zone 21 (MP21; Rupelian; Fig. 1; Solé et al., 2021). This locality is mainly

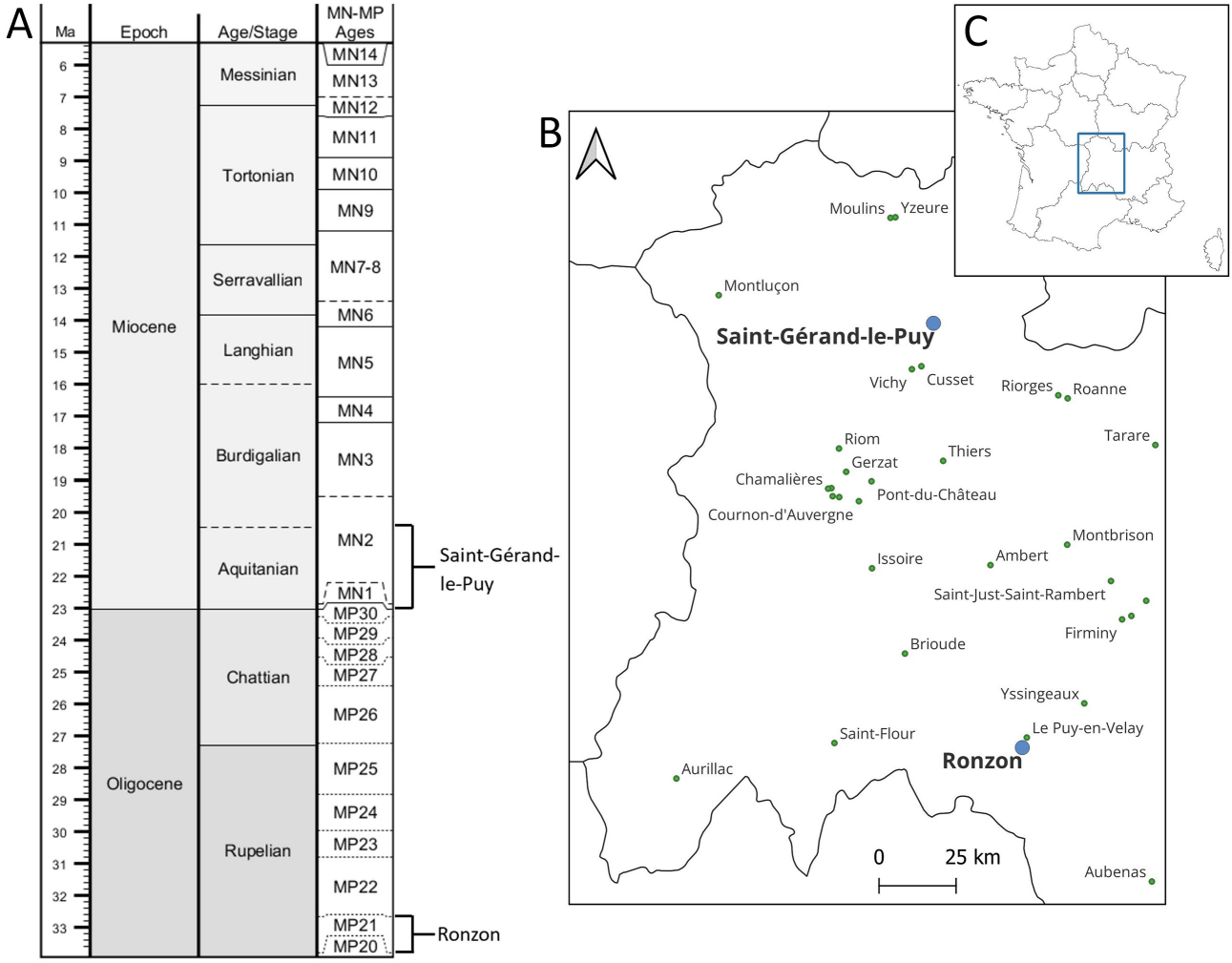

Figure 1. A. Age and mammalian Paleogene/Neogene zones for the fossil localities Saint-Gérand-le-Puy and Ronzon in the Oligocene and Miocene. Adapted from time scale creator https://timescalecreator.org/index/index.php according to GTS 2020. Ages of localities: Göhlich & Mourer-Chauviré, 2005; Solé et al., 2021. Abbreviations: MN, Mammal Neogene (zone); MP, Mammal Paleogene (zone). **B.** Map of the fossil localities Saint-Gérand-le-Puy and Ronzon in France. Background data from https://simplemaps.com (outlines France, CC BY 4.0) and https://www.geofabrik.de/ (cities, CC BY-SA 2.0). **C**. Inset showing location in France.

known for the abundant mammalian fossils found in calcareous sediments (Turland et al., 1993). *Diplocynodon* remains have also been described from this locality (Berg, 1966), attributed to *Diplocynodon "gervaisi"*, now considered an invalid taxon (Martin, 2010; Rio et al., 2020). *Diplocynodon* was already known from this locality when Filhol himself studied the fossils from Ronzon (Filhol, 1881).

2.2. Methods

As part of the study of crocodylian fossils within the Filhol collection at KU Leuven, a systematic process was undertaken to sort, clean, photograph, and catalogue the specimens. The examination began with an assessment of all material of the Filhol collection of KU Leuven previously labelled as "*Diplocynodon*" or "Crocodylia". A rough categorization of disarticulated bones was conducted, grouping similar types of bones such as coracoids, premaxillae, osteoderms, and vertebrae together. The rest of the collection was then scrutinized to locate similar bones. Despite finding some misplaced items such as a cast of a primitive amphibian and hollow bird bones, no additional Crocodylia remains were discovered.

All specimens were cleaned using water, dish soap, soft brushes, and toothbrushes. The larger marl tablets from Ronzon were cleaned with minimal water to maintain their structural integrity and to not damage previously applied glue. To prevent limescale from the tap water, all fossils were rinsed with demineralized water. The cleaned specimens were then dried in drying ovens at 35 °C to 37 °C for one to four days. Following the cleaning and drying process, polyvinyl acetate glue was used to repair fragmented pieces.

After washing and drying, a finer sorting according to anatomical position took place. The most complete and detailed specimens of each bone type were chosen, numbered, and photographed. Photographs were taken using three lightboxes to avoid shadows, a scale card, a grey background to reduce contrast, and a tripod-mounted Nikon D7500 camera with a VR Af-S 18-140 mm 1:3.5-5.6 GED lens for normal photographs and a Sigma 105mm F/2.8 EX DG Macro OS lens for details. Kneadable erasers and boxes were used to position the specimens in a way that preserves optical and spatial information. The photographs were edited using Adobe Photoshop 2020 version 21.0.1 to remove backgrounds, add a digital scale bar, and lighten shadows to enhance detail.

A comprehensive list of all *Diplocynodon* material in the Filhol collection was created (Table 2). The final step involved assigning the remains to specific genera and species by comparing

them to scientific literature. This categorization was performed separately for both localities.

2.3. Material

About 800 fragments attributed to Crocodylia have been recovered from the Filhol collection, of which about a quarter was accompanied by details on the provenance. Seventy anatomically representative fragments are figured (Figs 2–23).

Material from Ronzon remains embedded in the sediment matrix, of which there are 17 pieces (Figs 24–34). All fragmentary material that retained locality information originates in Saint-Gérand-le-Puy, and all other fragments in the collection exhibit similar preservation. In general, the bones are yellowish-brown in colour, relatively hard and partially covered in yellow-white sand. Specimens display a varying degree of preservation, often broken into parts or with brittle structure, but a sizable number show a good degree of preservation.

A total of 781 crocodylian specimens are present in the entire Filhol collection of the KU Leuven. Out of the specimens from Saint-Gérand-le-Puy, the majority (400) belongs to the axial skeleton, consisting of vertebrae (150), ribs (50) and fragments of mandible and skull (200). A total of 78 specimens are part of the appendicular skeleton. The remainder of the specimens are osteoderms (235). These large numbers, however, give an inflated impression of the amount of scientifically useful material in the collection, as most of the specimens are small, fragmentary remains (Table 2). This list is ordered by locality and type of bone.

2.4. Assumptions

For the determination of the material of the Filhol collection some assumptions and restrictions had to be established. The first assumption is that all unlabelled, loose bones in the collection were found at Saint-Gérand-le-Puy. This assumption was made on the basis that labelled and unlabelled specimens were stored together in the same boxes and that the labels within these boxes all indicate that the collection contains *Diplocynodon* (*ratelii*) from Saint-Gérand-le-Puy. Specimens from Ronzon were labelled separately. Moreover, the loose specimens and the labelled specimens were preserved in a similar manner; they are alike in colour and contain remains of a similar matrix, a loose sandy substrate. Given that *Diplocynodon ratelii* is the only species consistently recovered from Saint-Gérand-le-Puy and the Aquitanian (Vaillant, 1872; Bucher et al., 1985; Martin, 2010), the second assumption is that all disarticulated bones which are clearly identifiable as crocodylian and have the same stratigraphic age belong to the same species and therefore show characteristics that must be uniform to the species in question.

2.5. Anatomical abbreviations

alp, anterolateral process; an, angular; ap, anterior process; apd, anterior peduncle; apl, anterior posterior length; arp, acromion process; at, anterior tip; asc, anterior semicircular canal; cbl, coracoid blade; cft, coracoid shaft; chd, coracoid head; co, condyle; cqp, cranioquadrate passage; cr, cochlear recess; ctr, centrum; dcr, deltoid (acromial) crest; del, descending lamina; den, dentary; diap, diapophysis; dib, distal blade; dlp, dorsolateral process; dol, dorsal lamina; dor, dorsal; dpc, deltopectoral crest; dph, diaphysis; ds, deep sulcus; emf, external mandibular fenestra; eph, epiphysis; eps, ectopterygoid-pterygoid suture; es, endocranial surface; f, frontal; fa, foramen aëreum; fi, fibula; fic, foramen intermandibularis caudalis; fm, femur; fmh, femoral head; fo, foramen; fp, fronto-parietal suture; fs, frontal step; fte, musculus femorotibialis externus; fti, musculus flexor tibialis internus; gf, glenoid fossa; gl, gastrolith; glfc, glenoid facet; glp, glenoid lip; hap, hypapophysis; il, ilium; ipr, intertympanic pneumatic recess; itf, infratemporal fenestra; jg, jugal; jga, jugal arch; lb, long bone; ll, lateral lobe; lmk, longitudinal midline keel; ltf, laterotemporal fenestra; mc, metacarpal; mds, musculus dorsalis scapulae; ml, medial lobe; mld, musculus latissimus dorsi; mf, Meckelian fossa; mfdl, musculus flexor digitorum longus; mph, metaphysis; mppc, medial pharyngeal pneumatic canal; mpt, musculus pronator teres; mt, metatarsal; mtm, musculus teres major; mx, maxilla; no, notch; nrc, neural canal; nrs, neural spine; o, orbit; oc, occipital condyle; olp, olecranon process; os, otoccipital suture; ost, osteoderm; p, parietal; paa, parapophysis; pas, parabasisphenoid suture; patp, preacetabular process; pbr, peduncle bridge; pd, peduncle; pdp, posterodorsal process; phc, pharyngotympanic canal; pit, musculus puboischio tibialis; pm, posterior margin; po, postorbital; pob, postorbital bar; potp, postacetabular process; pozap, postzygapophysis; pp, posterior process; ppd, posterior peduncle; pr, pneumatic recess; pzap, prezygapophysis; prs, prootic suture; psc, posterior semicircular canal; qjg, quadratojugal; rap, retroarticular process; ri, ridge; sa, scapula; sbl, scapular blade; sc, sagittal crest; shd, scapular head; sft, shaft; soc, supraoccipital; socs, supraoccipital suture; spl, splenial; sq, squamosal; stf, supratemporal fenestra; sur, surangular; sut, suture line; svt, sacral vertebra; t, tuberosities; too, tooth; trr, transverse ridge; ur, utricular recess; vbp, ventral basioccipital plate; vmp, ventromedial process; vt, vertebra; vtr, ventral.

2.6. Catalogue numbers

All specimens from Saint-Gérand-le-Puy are collectively catalogued in the KU Leuven vertebrate palaeontological collection under the number PLV1983. In recent years, most specimens from this collection have also received a second identifier, in a new catalogue system for the KU Leuven palaeontological collections, set up under DiSSCO-Flanders (Van Baelen et al., 2022). In this system, identifiers all have the form PALxxxx, with x being numbers (Table 2). Each number is used for a different number of specimens. For unique identification for specimens studied in this study, here a third number was added to all photographed and described specimens in the form of KUL-Fxxx (Figs 2–23). The specimens from Ronzon are only identified by the KUL-Fxxx catalogue number (Figs 24–34).

3. Palaeontological determinations

3.1. Recognised species

Unranked clade Eusuchia Huxley, 1875, sensu Brochu, 2003
Order Crocodylia Gmelin, 1789, sensu Benton & Clark, 1988
Superfamily Alligatoroidea Gray, 1844, sensu Brochu, 2003
Family Diplocynodontinae Brochu, 1999
Genus *Diplocynodon* Pomel, 1847

Type species. *Diplocynodon ratelii* Pomel, 1847.

***Diplocynodon ratelii* Pomel, 1847**

Referred specimens. We refer 764 specimens to *Diplocynodon ratelii* of which 200 cranial specimens, 513 postcranial specimens and 51 undetermined specimens. All specimens are disarticulated except for some parts of the cranial. These

Table 2. List of all *Diplocynodon* material in the KU Leuven Filhol collection. When the locality was not explicitly specified on the container, it is assumed to be from Saint-Gérand-le-Puy.

Object	Amount	Locality	Catalogue numbers
coracoid	8	*not specified*	PLV1983, PAL3450
ischium	5	*not specified*	PLV1983
pubis	5	*not specified*	PLV1983, PAL3450
scapula	4	*not specified*	PLV1983, PAL2050
ilium	3	*not specified*	PLV1983
mandibula	42	*not specified*	PLV1983, PAL3450
maxilla	21	*not specified*	PLV1983, PAL3450
indeterminate fragments of mandibula and maxilla	*50*	*not specified*	*PLV1983*
premaxilla	2	*not specified*	PLV1983, PAL3450
basioccipital	3	*not specified*	PLV1983, PAL3450
parietal	2	*not specified*	PLV1983
jugal	11	*not specified*	PLV1983
palatine	1	*not specified*	PLV1983, PAL3450
skull table	4	*not specified*	PLV1983, PAL3450
articular	5	*not specified*	PLV1983, PAL3450
quadrate	6	*not specified*	PLV1983, PAL3450
ectopterygoid	18	*not specified*	PLV1983, PAL2029/PAL2027
tooth	16	*not specified*	PLV1983, PAL3450/PAL3461
skull fragment, >4 cm	3	*not specified*	PLV1983, PAL3450/PAL3509
skull fragment, <4 cm	8	*not specified*	PLV1983
vertebra	144	*not specified*	PLV1983, PAL2042/PAL2043/PAL2046
sacral vertebra	2	*not specified*	PLV1983
caudal vertebra	2	*not specified*	PLV1983, PAL2048
humerus	7	*not specified*	PLV1983, PAL3597
femur	10	*not specified*	PLV1983, PAL3517
fibula	4	*not specified*	PLV1983, PAL3509
radius	4	*not specified*	PLV1983, PAL3509
ulna	2	*not specified*	PLV1983, PAL3509
metatarsal/metacarpal	15	*not specified*	PLV1983, PAL3509
phalange	10	*not specified*	PLV1983, PAL3509
osteoderm	92	*not specified*	PLV1983, PAL3519
costa	50	*not specified*	PLV1983, PAL3515
undetermined elongated bone fragment	*13*	*not specified*	*PLV1983*
undetermined other bone fragment	*5*	*not specified*	*PLV1983*
undetermined fragment (Diplocynodon)	*3*	*not specified*	*PLV1983*
box of bone shards	*3*	*not specified*	*PLV1983*
skull fragment	8	Saint-Gérand-le-Puy (FR)	PLV1983
vertebra	2	Saint-Gérand-le-Puy (FR)	PLV1983
metatarsal/metacarpal	1	Saint-Gérand-le-Puy (FR)	PLV1983, PAL3509
osteoderm	143	Saint-Gérand-le-Puy (FR)	PLV1983, PAL3519
bone fragment	*2*	*Saint-Gérand-le-Puy (FR)*	*PLV1983*
stone fragment	*25*	*Saint-Gérand-le-Puy (FR)*	*PLV1983*
mandibula in matrix	1	Ronzon (FR)	
maxilla in matrix	1	Ronzon (FR)	
bone fragments in matrix	12	Ronzon (FR)	
osteoderms, vertebrae, scapula, ilium and other bone fragments in matrix	1	Ronzon (FR)	
osteoderms and bone fragments in matrix	1	Ronzon (FR)	
bag of tiny <1 cm bone fragments	*1*	*Ronzon (FR)*	
Total	**781**		

specimens are contained under the catalogue numbers PLV1983, PAL2027, PAL2029, PAL2042, PAL2043, PAL2046, PAL2048, PAL2050, PAL3450, PAL3461, PAL3509, PAL3515, PAL3517, PAL3519, PAL3597 and KUL-F1 up to and including KUL-F58 and KUL-F70.

Locality and age. All specimens come from Saint-Gérand-le-Puy in France from the Aquitanian (23–20.4 Ma; Göhlich & Mourer-Chauviré, 2005).

Crocodylia indet. Gmelin, 1789, sensu Benton & Clark, 1988

Referred specimens. We refer 17 specimens to Crocodylia indet. including both cranial and postcranial elements. Some specimens are articulated and all are embedded in stone. These specimens have the catalogue numbers KUL-F59 up to and including KUL-F69.

Locality and age. All specimens come from Ronzon in France from the early Rupelian (33.9–32.5 Ma; Solé et al., 2021).

3.2. Description of selected specimens from Saint-Gérand-le-Puy

3.2.1. Cranial table

Two hundred skull fragments have been recovered, of which seven were photographed. Specimen KUL-F28 (Fig. 2A) is incomplete, but preserved in its original state, while specimen KUL-F50 (Fig. 2B) is relatively complete but has been reassembled. Specimen KUL-F4 (Fig. 2D) has also been reassembled, but shows a high degree of preservation. In all cases, deformation is minimal.

The cranial table is covered in pits that generally show a rounded or slightly elongated shape (Fig. 2). In dorsal view, the squamosal is T-shaped and narrows gradually towards the anterior end where it sutures diagonally (medial closer to posterior, lateral closer to anterior) with the postorbital (Fig. 2B, D). The postorbital is curved and maintains the same width as the anterior squamosal. It connects to the frontal with a medially inclined suture. The frontal gradually narrows anteriorly but widens at the anterior end (in dorsal view), without reaching the same width as in the posterior end (Fig. 2B, C). The frontal is markedly concave and shows a dorsoventral step on the posterior part at its maximum mediolateral width, as well as on the anterior process. It shows no midsagittal crest.

The parietal is well preserved and posterolaterally sutures linearly with the squamosal and anteriorly with the frontal in a concavoconvex shape (Fig. 2B, D). The parietal has the same width on the posterior and anterior margins, but it narrows in the middle where it delineates the medial margin of the supratemporal fenestrae. The supratemporal fenestrae are rather long and open and not very wide (Fig. 2B). The ratio of maximum mediolateral width to maximum anteroposterior length of the supratemporal fenestrae being 0.665 ± 0.0056 and the ratio of the anteroposterior supratemporal fenestra length to the anteroposterior cranial table length being 0.566 ± 0.023. The supratemporal fenestrae are intersected by the frontoparietal suture. There is no sagittal crest between the fenestrae, no fossa in the anteromedial corner and no foramina in the parietal, medial wall.

Remarkably, the posterior endocranial surface of the parietal and supraoccipital is well preserved and attached to each other, so that it is possible to see a variety of openings that would normally be hidden within the rest of the skull (Fig. 3). Parts of the intertympanic pneumatic recess are visible going into the parietal (in ventral view). Also, two foramina are visible in the anterior lamina of the supraoccipital (Fig. 3C). Multiple different sutures are well preserved, including the frontoparietal suture, prootic suture and supraoccipital suture. In the supraoccipital the anterior and posterior semicircular canals, foramina for external occipital veins and the utricular recess are preserved.

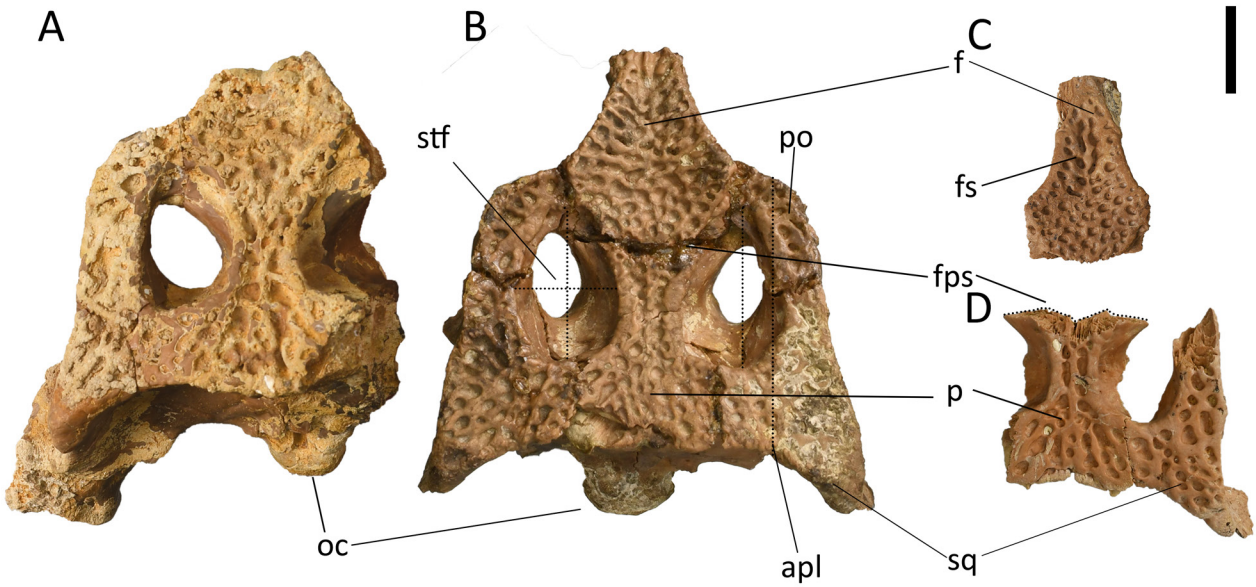

Figure 2. Cranial table specimens of *Diplocynodon ratelii* all in dorsal view (PLV1983, PAL3450). **A.** Partial cranial table with occipital condyle (KUL-F28). **B.** Complete cranial table with occipital condyle (KUL-F50). **C.** Isolated frontal (KUL-F18). **D.** Parietal and squamosal (KUL-F4). Provenance: Saint-Gérand-le-Puy. Scale bar = 1 cm. Anatomical abbreviations: see section 2.5.

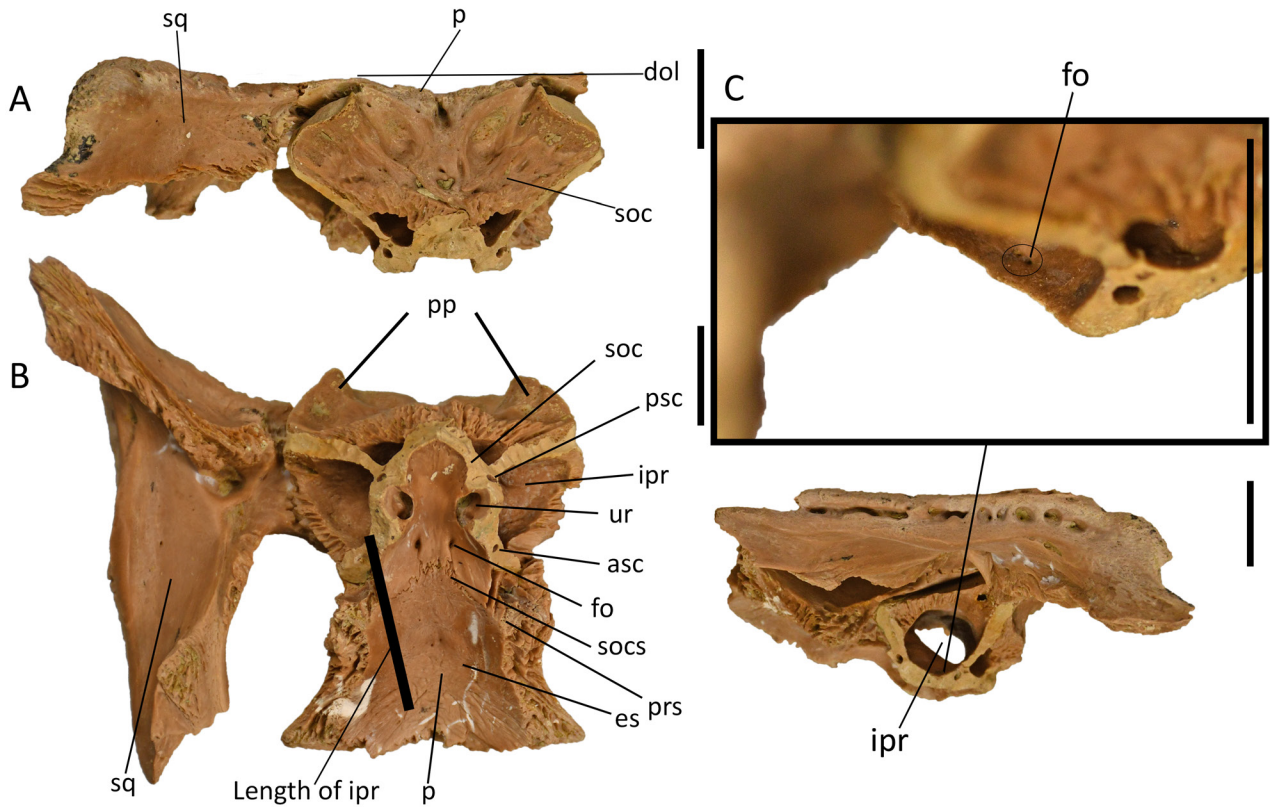

Figure 3. Well preserved parietal, squamosal and supraoccipital of *Diplocynodon ratelii* (PLV1983, PAL3450, KUL-F4). **A.** Posterior view. **B.** Ventral view with foramina for external occipital veins. **C.** Left lateral view with zoom-in on two foramina in the anterior lamina of the supraoccipital. Provenance: Saint-Gérand-le-Puy. Scale bar = 1 cm. Anatomical abbreviations: see section 2.5.

The basioccipital is very well preserved (Fig. 4). The tuberosities on the ventral surface are not very prominent (Fig. 4 A). The ratio of the maximum mediolateral width of the basioccipital plate to that of the condyle is smaller than 2 (1.7–1.9), indicating a rather narrow shape. The lateral margins of the ventral basioccipital plate are ventrally convergent. There is a sagittal crest on the ventral plate. In lateral view, the dorsoventral height of the ventral plate exposed below the occipital condyle is greater than the occipital condyle height (~1.7; Fig. 4B). The part between the occipital condyle and the anterior process is strongly curved dorsally on the ventral side and is completely flat on the dorsal endocranial surface as seen in lateral view. The endocranial surface itself is smooth and depressed ventrally, while the otoccipital sutures are flanked both laterally and medially by transverse ridges as seen in dorsal view (Fig. 4D). The anterior sutural surface is strongly rugose with ridges in the dorsoventral direction (Fig. 4 C). There is a prominent medial pharyngeal pneumatic canal which is connected to the pneumatic recess. This is flanked by a pharyngotympanic canal laterally. The ventral margin of the basioccipital is slightly concave.

3.2.2. Ectopterygoid

Eighteen ectopterygoids have been recovered. The dorsolateral process is longer and thinner than the ventromedial process, which is bladed and more massive (Fig. 5). There is a high degree of rotation between the dorsolateral and the ventromedial process. The anterior tip of the dorsolateral process is acute and unforked. The anterior margin of the ventromedial process is pierced by at least two large foramina. The ectopterygoid-pterygoid suture is straight. The extent of the ectopterygoid relative to its adjacent bones cannot be determined.

3.2.3. Quadrate

Only the posterior part of the quadrate is preserved and the posterodorsal process is fractured (Fig. 6). The ventral surface is smooth while the dorsal surface is rough. The size of the foramen aëreum is small, with a diameter of less than half of the dorsoventral height of the medial hemicondyle and its position is on the dorsal surface of the posterior ramus as seen in dorsal view. The lateral part of the condyle is larger than the medial part, which is ventrally reflected. There is a notch on the dorsal articular border, which covers about a third of the mediolateral width of the quadrate condyle.

3.2.4. Maxilla and premaxilla

The premaxilla has five teeth, and it has prominent notches from the dentary teeth (Fig. 7B). The 3rd and 4th alveoli are the largest, and they are approximately equal in size. The position of the penultimate premaxillary alveolus relative to the antepenultimate alveolus is posterolateral, and more generally, the alveoli are arched in a posterolateral line. The 2nd alveolus is separated from the 1st and close to the 3rd. In lateral view, the contour of the external naris has a crest-like thickening in the posterior part which lines off the margin of the external naris up to the premaxillary suture (Fig. 7A).

Twenty-one maxilla fragments were preserved. We assume that specimen KUL-F48 in Figure 7D is complete where it meets the premaxilla, based on the preservation and the posterior

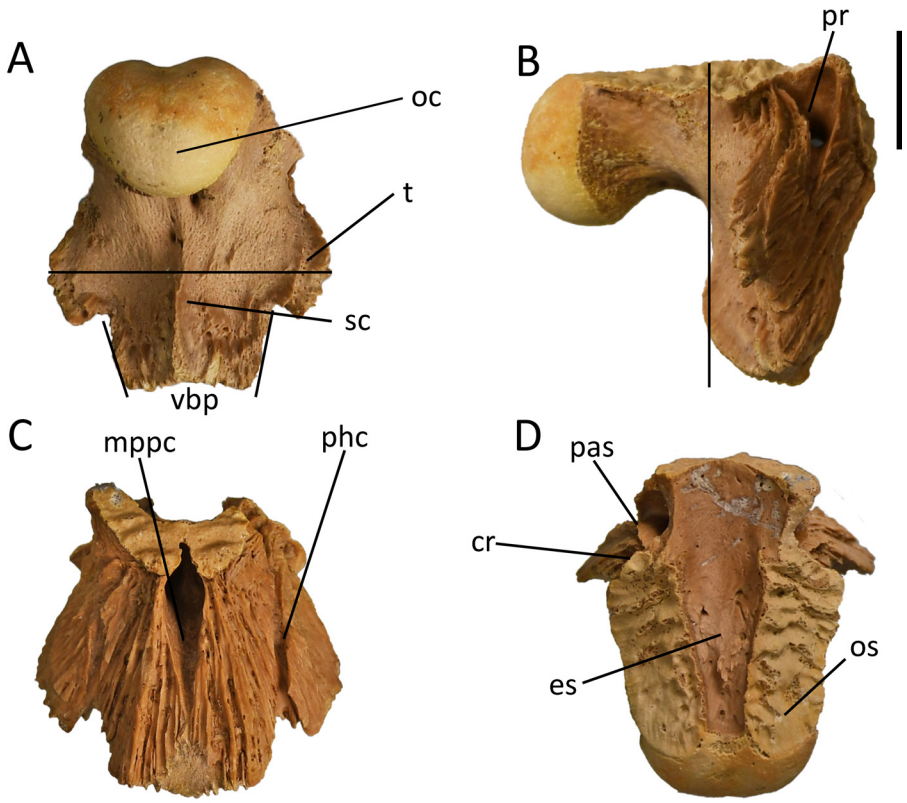

Figure 4. Isolated basioccipital of *Diplocynodon ratelii* (PLV1983, PAL3450, KUL-F5). **A.** Posteroventral view, maximal mediolateral width is narrow indicated by horizontal line. **B.** Right lateral view, dorsoventral height of the ventral plate indicated by vertical line. **C.** Anterior view. **D.** Dorsal view. Provenance: Saint-Gérand-le-Puy. Scale bar = 1 cm. Anatomical abbreviations: see section 2.5.

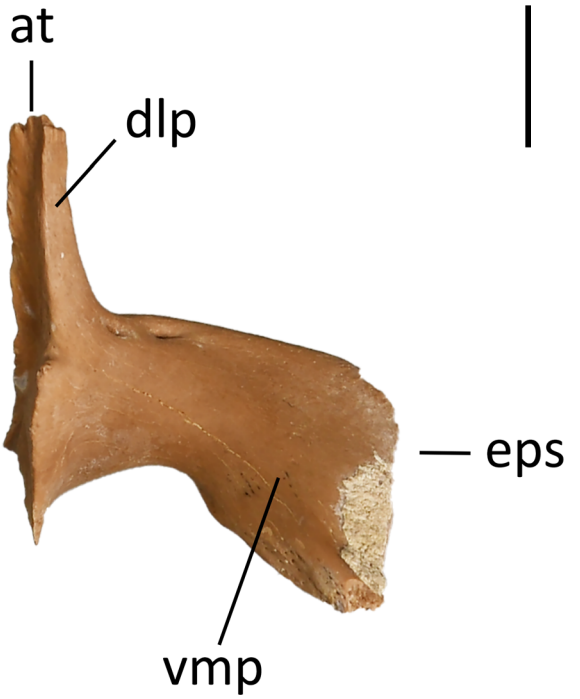

Figure 5. Isolated ectopterygoid of *Diplocynodon ratelii* in ventral view (PLV1983, PAL2027, KUL-F11). Provenance: Saint-Gérand-le-Puy. Scale bar = 1 cm. Anatomical abbreviations: see section 2.5.

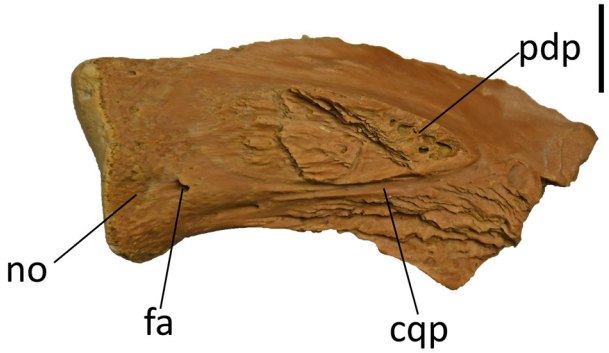

Figure 6. Isolated quadrate of *Diplocynodon ratelii* in dorsal view (PLV1983, PAL3450, KUL-F7). Provenance: Saint-Gérand-le-Puy. Scale bar = 1 cm. Anatomical abbreviations: see section 2.5.

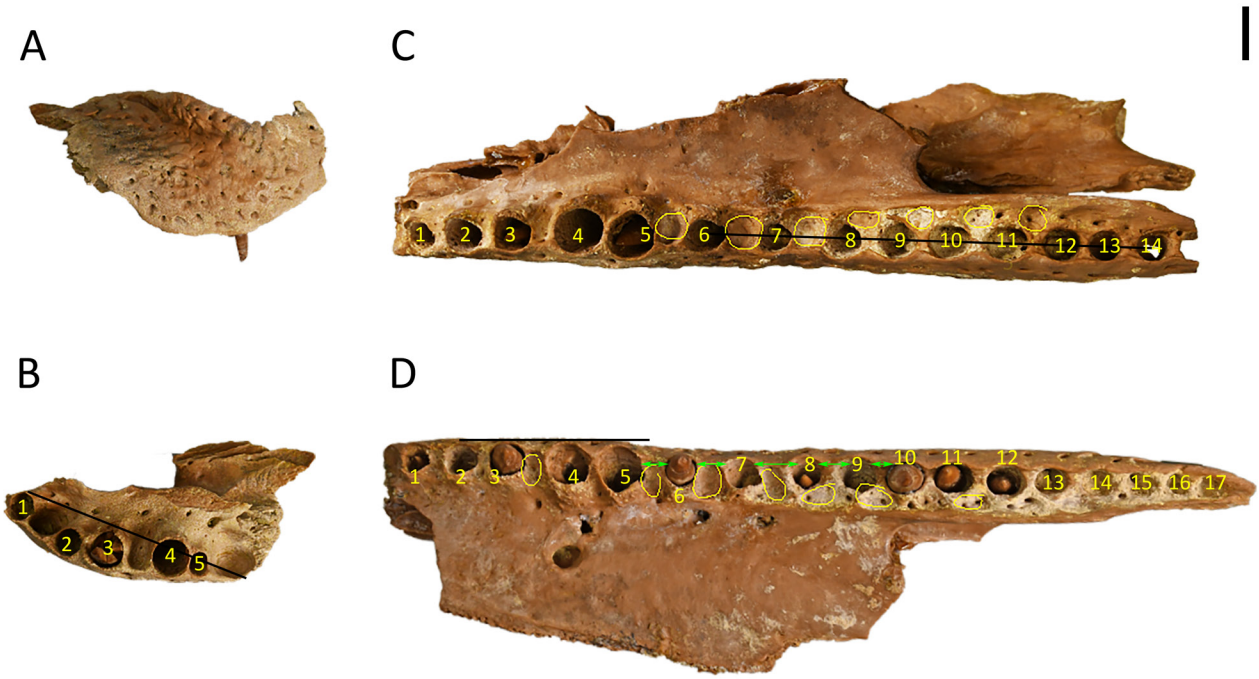

Figure 7. Maxilla and premaxilla specimens (PLV1983, PAL3450) with marked alveoli positions. **A–B.** KUL-F31, right premaxilla in right dorsolateral view (A) and ventral view (B) with the posterolateral arch in the premaxillary alveoli marked by the black line. **C.** KUL-F49, right maxilla in ventral view with the posterior linear toothrow marked by a black line, partial interlocking of occlusion pits marked by yellow circles. **D.** KUL-F48, left maxilla in ventral view with the straight anterolateral margin marked by the black line, the occlusion pits marked by yellow circles and posteriorly narrowing interalveolar distance marked by green arrows. Provenance: Saint-Gérand-le-Puy. Scale bar = 1 cm.

narrowing of the tooth row and a complete comparison with fragmentary pieces. The ratio of maximum dorsoventral height of the maxilla to mediolateral width of the maxilla at the 5th maxillary alveolus is 0.6, indicating a dorsoventrally tall rostrum. The complete left maxilla has 17 alveoli (Fig. 7D). The 4th and 5th alveoli are not confluent but very close and only separated by a thin septum. They are both notably enlarged, comprising the largest maxillary alveoli. The posterior teeth are largely equal in size, and only the first tooth is smaller. The interalveolar distance between the 1st and the 10th alveoli is smaller than the diameter of the 1st alveolus, and most alveoli are evenly spaced. The lateral profile between the 1st and the 5th alveoli is straight and there is no widening bulge adjacent to the largest alveoli. The posterior tooth row is linear. There is a partial interlocking of occlusion pits, which means that occlusion pits of dentary teeth can be found both between alveoli and next to them. There is no significant diastema between the 5th and the 6th alveoli. The spacing between the 6th and the 8th alveoli is wider due to occlusion pits. The alveoli are circular, even posteriorly.

3.2.5. Dentary and splenial

Forty-two mandible fragments were recovered. The first dentary alveolus projects anterodorsally as seen in dorsal view (Fig. 8B). The 3rd and 4th alveoli are confluent (Fig. 8A, B). The dorsoventral height of the mandible at the level of the 1st to the 4th alveoli relative to the 11th and 12th alveoli is slightly higher (Fig. 8C). The shape of the dorsal profile between the 4th and the 10th alveoli in lateral view is curved. The largest alveoli posterior to the 4th dentary alveolus are the 10th and 11th (Fig. 8A). The dentary symphysis extends to the fourth alveolus. The extent of the splenial cannot be determined in any specimens. The shape of the posterior margin of the dentary symphyseal surface in medial view has the dorsal lobe extending further posterior than the ventral lobe (Fig. 8D). The orientation of the posteriormost alveoli is in a straight line (Fig. 8E).

3.2.6. Teeth

Sixteen loose teeth were recovered from the collection, two of which (KUL-F45, KUL-F43) were photographed (Fig. 9). These teeth were chosen as KUL-F45 is the largest tooth in the collection and KUL-F43 is one of the best-preserved most representative specimens. Additionally, several jaw parts contain parts of teeth and even replacement teeth growing inside older teeth. The teeth are generally circular in cross section and there are no obvious carinae or serration.

3.2.7. Articular

The articular projects posterodorsally at an angle of 30°, which indicates a rather flat shape (Fig. 10). At the articular, the position of the foramen aëreum is inset from the medial margin of the retroarticular process and there is no lamina. The retroarticular process does not have a crest. There is a sharp division between the retroarticular process and the glenoid fossa. There is no anterior process of the articular on the posterior wall of the adductor chamber.

3.2.8. Angular

The angular and its fragments are covered in deep pits laterally and are fully smooth medially (Fig. 11). There is a deep sulcus on the dorsal surface, and it has three large and two small nerve openings on the posterodorsal surface. The medioventral surface also has four nerve openings with approximately equal spacing. The angular participates in both the external mandibular fenestra with a moderate concavity and the foramen intermandibularis caudalis with a strong concavity.

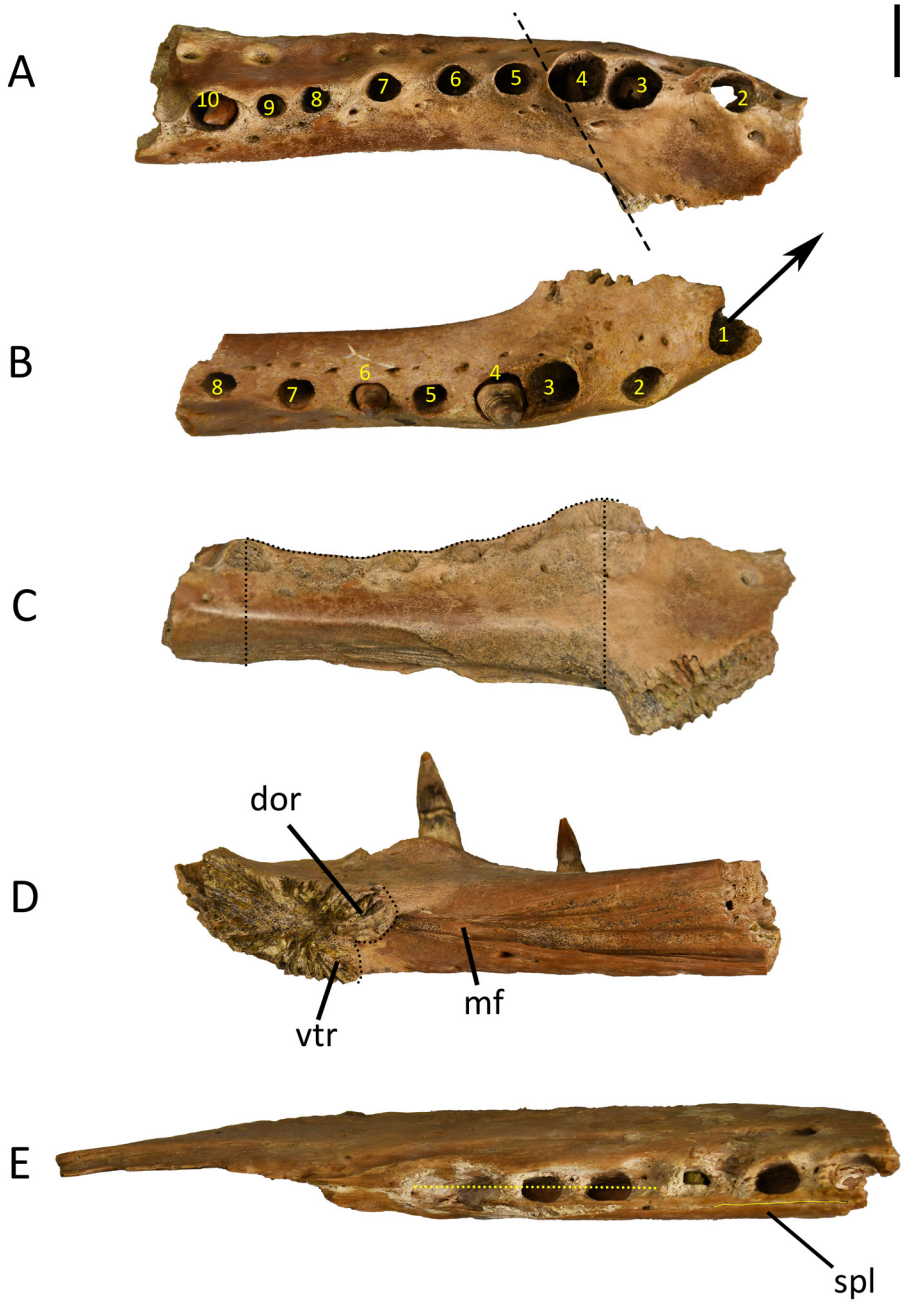

Figure 8. Mandibular specimens of *Diplocynodon ratelii* (PLV1983, PAL3450) with marked alveoli positions. **A, C.** KUL-F44, anterior part of left dentary. **B, D.** KUL-F42, anterior part of right dentary. A, dorsal view, extent of symphysis marked by the black line; B, dorsal view, projection of first alveolus marked by the arrow; C, medial view, dorsoventral extent and curved outline marked by the black lines; D, medial view; **E.** dorsal view, straight line of alveoli is marked with the black line (KUL-F52). Provenance: Saint-Gérand-le-Puy. Scale bar = 1 cm. Anatomical abbreviations: see section 2.5.

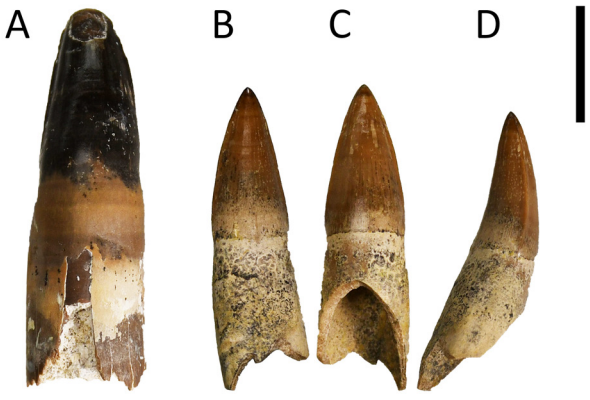

Figure 9. Isolated teeth of *Diplocynodon ratelii* (PLV1983). **A.** KUL-F45 (PAL3461); **B–D.** KUL-F43 (PAL3450) figured in lingual (B), labial (C), and anterior (D) view. Provenance: Saint-Gérand-le-Puy. Scale bar = 1 cm.

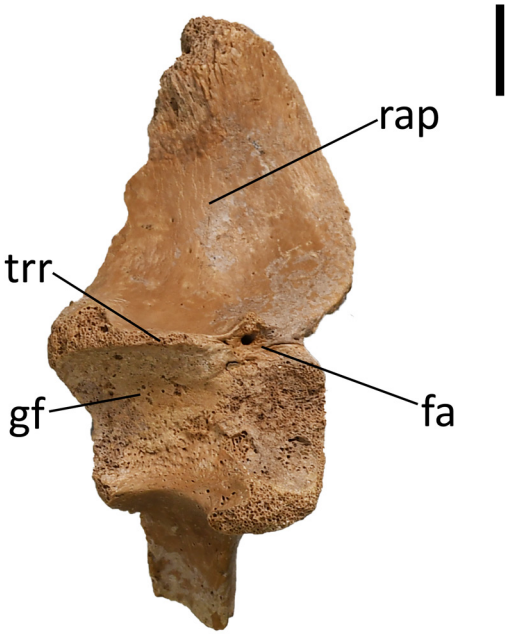

Figure 10. Isolated articular of *Diplocynodon ratelii* in dorsal view (PLV1983, PAL3450, KUL-F26). Provenance: Saint-Gérand-le-Puy. Scale bar = 1 cm. Anatomical abbreviations: see section 2.5.

3.2.9. Jugal

The jugal is covered in deep large pits laterally and is smooth medially (Fig. 12). The postorbital bar is oriented perpendicular to the anteroposterior axis of the jugal and there is no significant posterodorsal foramen towards the infratemporal fenestra. The jugal arch is moderately concave.

3.2.10. Palatine

The paired palatine is filled with a large paired hollow cavity, the nasopharyngeal ducts (Fig. 13). There is a strong lateral flare posteriorly (also including the pterygoids) with a linear palatine-pterygoid suture. The anterior process is broken.

3.2.11. Vertebrae

One hundred and fifty specimens represented vertebrae, either partially or completely preserved (Fig. 14). All vertebrae are isolated and most are procoelous, the only exception being a biconvex first caudal vertebra (KUL-F14, Fig. 14M–P).

The cervical vertebra as shown on Figure 15 is procoelous. The posterior condyle bends slightly dorsally as seen in lateral view. The cervical hypapophysis is present, it is unforked and located towards the anterior part of the centrum with vertical implantation, but the anterior margin curves slightly in posterior direction. It is flanked by paired parapophyses. As seen in anterior view, the diapophyses are curved downward and are comparatively short. The outline of the neural canal is approximately square. The prezygapophysis is more acute than the postzygapophysis. The anterior margin of the prezygapophysis is anterior to the level of the anterior extent of the hypapophysis. The neural spine is inclined posteriorly and is 1/3 of the total dorsoventral and anteroposterior extent of the cervical vertebra. In anterior/posterior view it is rod-like, but in lateral view it thickens in anteroposterior direction.

3.2.12. Osteoderms

Two hundred and thirty-five osteoderms were recovered from the collection. Ornamentation exists in the form of round pits with smooth margins and variable lengths and sizes (Fig. 16). A longitudinal midline keel is present in dorsal osteoderms (Fig. 16A), and absent in ventral osteoderms (Fig. 16B, C). It does not reach the anterior end. Dorsal osteoderms show variable

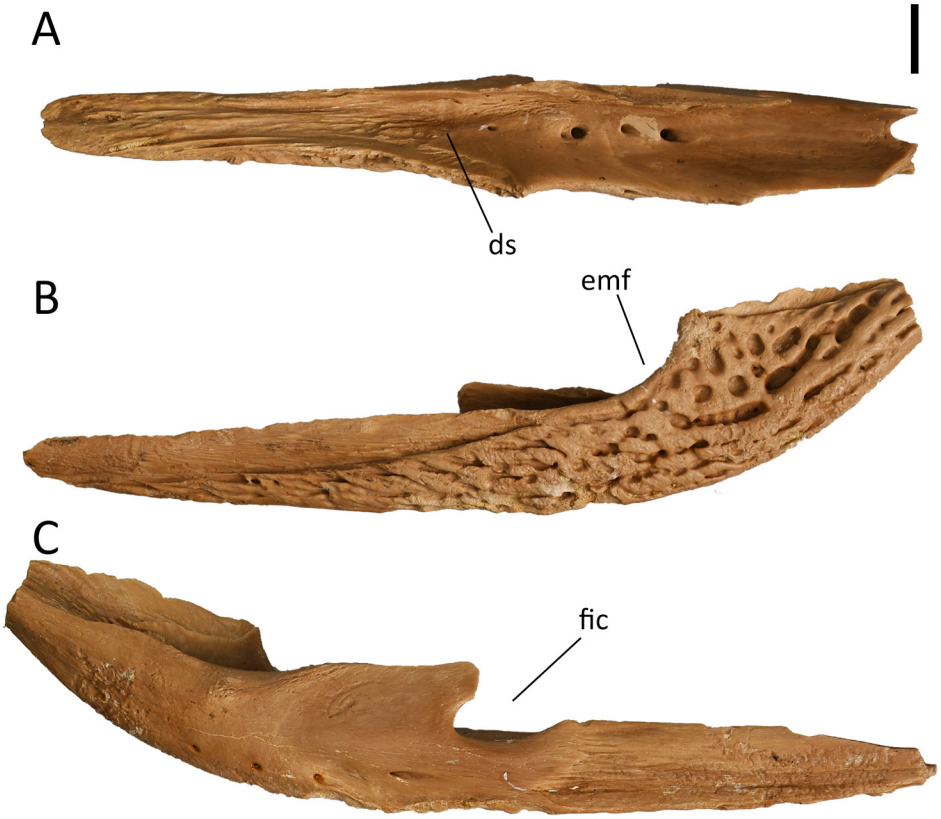

Figure 11. Isolated angular of *Diplocynodon ratelii* in dorsal (**A**), left lateral (**B**) and medial (**C**) view (PLV1983, PAL3450, KUL-F25). Provenance: Saint-Gérand-le-Puy. Scale bar = 1 cm. Anatomical abbreviations: see section 2.5.

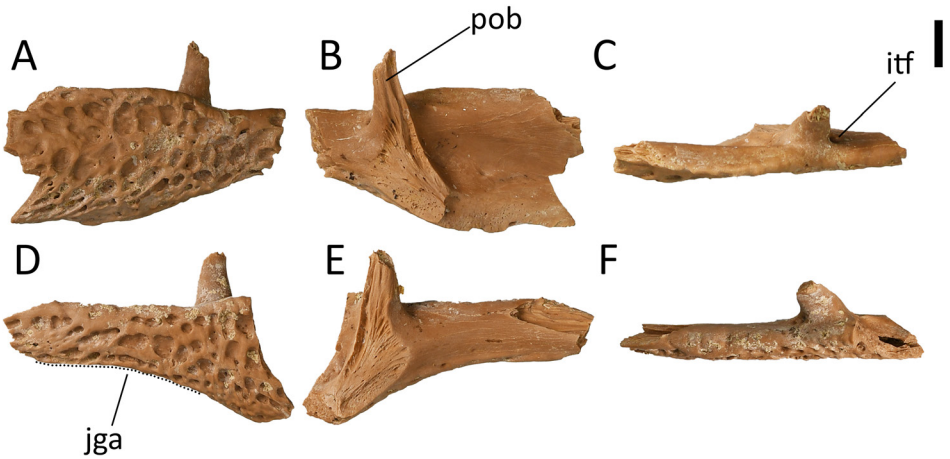

Figure 12. Isolated jugal specimens of *Diplocynodon ratelii* (PLV1983, PAL3450). **A–C.** KUL-F15A, left jugal in left lateral (A), medial (B), and dorsal view (C). **D–F.** KUL-F15B, right jugal in right lateral (D), medial (E), and dorsal view (F). Provenance: Saint-Gérand-le-Puy. Scale bar = 1 cm. Anatomical abbreviations: see section 2.5.

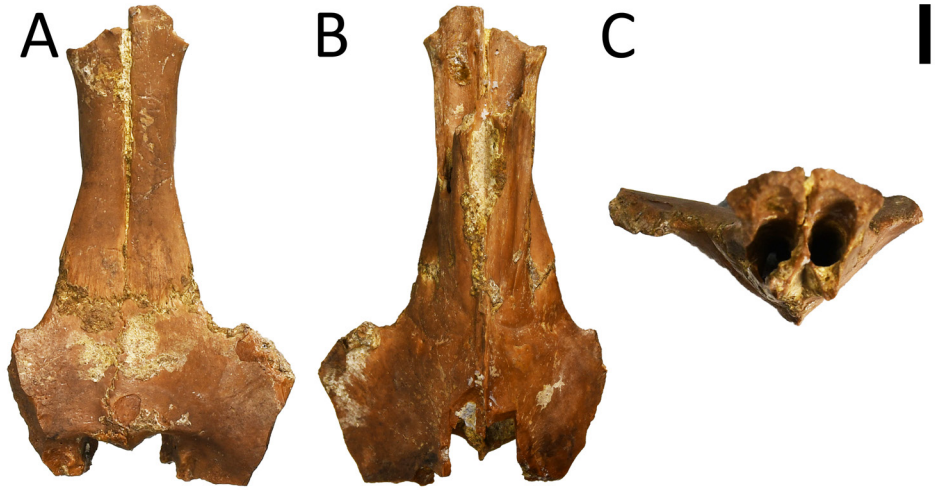

Figure 13. Palatine and (partial) pterygoids of *Diplocynodon ratelii* (PLV1983, PAL3450, KUL-F47) in ventral (**A**), dorsal (**B**) and posterior view (**C**). Provenance: Saint-Gérand-le-Puy. Scale bar = 1 cm.

length-to-width ratio, but are generally square, or less wide than long. However, the osteoderm in Figure 16A is slightly wider than long. An anterolateral process, a homologous swelling at the anterolateral margin of the osteoderm, is present. Ventral osteoderms are paired (bipartite), with a small anterior part that in ventral view is smooth on the anterior edge and sutures with the larger posterior part (Fig. 16B, C).

3.2.13. Scapula and coracoid

Four scapulae and eight coracoids were recovered from the collection. Additional fragments might be identified as scapulae or coracoids. In lateral view, the anterior edge of the scapula is straight, while the posterior edge is strongly concave (Fig. 17A). The scapular blade is flat mediolaterally and wider than the scapulacoracoid facet. The angle subtended by the anterior and posterior margins of the anteroposterior flare of the dorsal end of the scapular blade is larger than 35° when looking in lateral and medial views (38–50°; Fig. 17A, B). The deltoid crest is thin. The scapulocoracoid facet is broad immediately anterior to the glenoid fossa and it tapers anteriorly (Fig. 17C, E). The ratio of maximum expansion of the distal coracoid to the maximum proximo-distal coracoid length is larger than 0.5 (49–54%), indicating a slightly broad shape (Fig. 17D). The coracoid expands distally and the coracoid blade is wider than the coracoid head. The coracoid blade is slightly curved ventrally.

3.2.14. Forelimbs

Seven humeri and two ulnae were recovered. In medial view, the humerus shows an abrupt deltopectoral crest ventrolaterally (sensu Rio et al., 2020) (Fig. 18A). The axial rotation is low but more distally, it rotates ventrally and it has a slight lateral bulge in the middle. There is a single muscle scar on the proximodorsal surface for *Musculus dorsalis scapulae*/*M. latissimus dorsi* and *M. teres major* which insert on a common tendon (Fig. 18B).

The ulna shows an uncompressed olecranon process and is uncurved at the proximal end (Fig. 18C). The proximal condyle has two processes towards the middle and widens medially. In lateral view, the distal condyle is thinner in the middle and approximately equal medially and laterally. The lateral ridge is not very prominent. Four radiuses were also recovered. The radiuses have a slight curve towards the distal condyle seen in anterior view (Fig. 18D). The distal condyle is slanted with one side extending further. The proximal condyle is straight and is slightly thinner in the middle and larger on both sides.

3.2.15. Ilium

Three ilia were recovered from the collection of which two are shown (Fig. 19). The preacetabular process is rounded and not very prominent (Fig. 19A). The dorsal outline of the postacetabular process is only slightly concave without prominent indentation. The posterior margin of the postacetabular process is deep with anteroposterior length to dorsoventral height ratio <1.

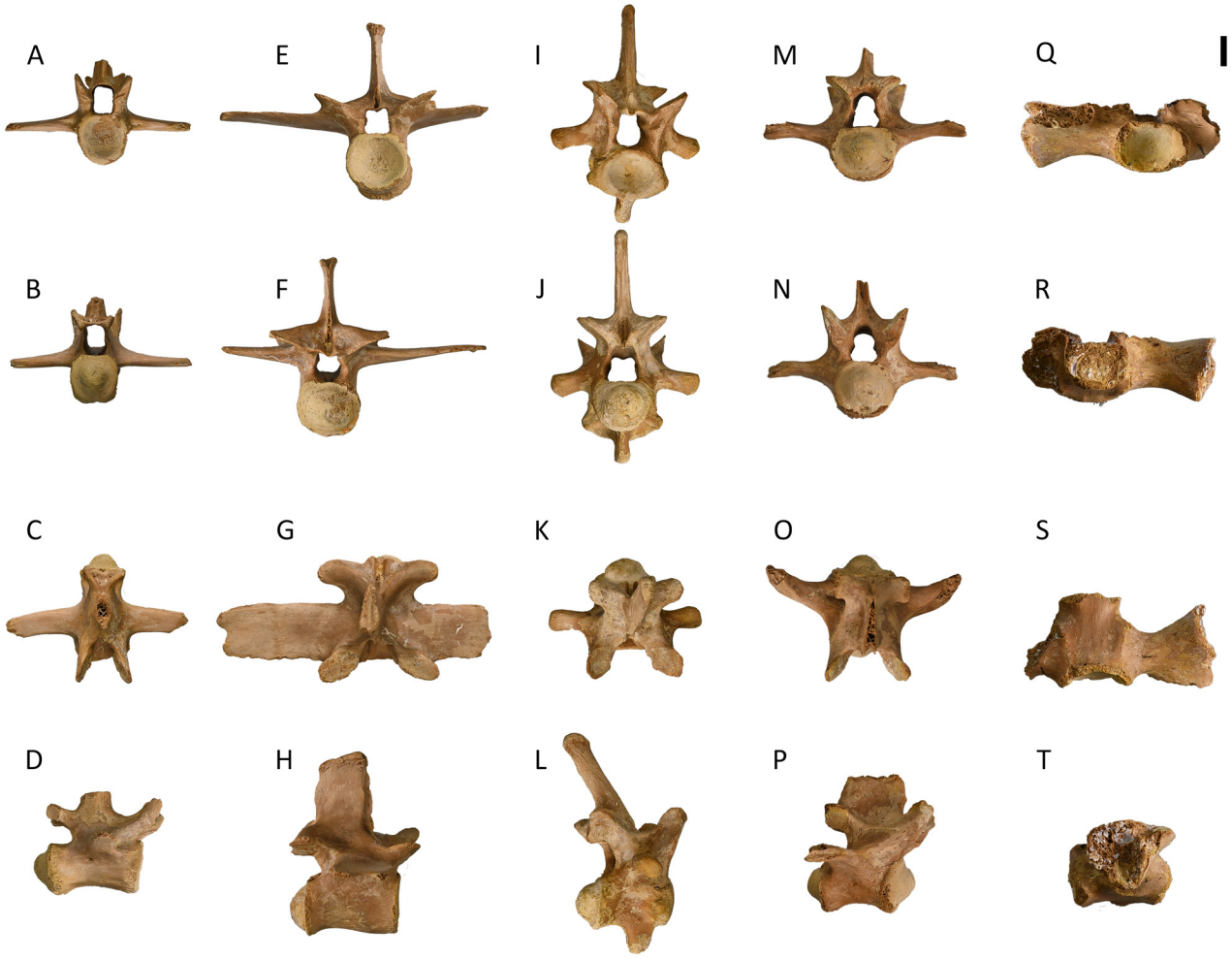

Figure 14. Isolated vertebrae of *Diplocynodon ratelii* (PLV1983). **A–D.** KUL-F10 (PAL2042), dorsal vertebra in posterior (A), anterior (B), dorsal (C), and right lateral view (D). **E–H.** KUL-F12 (PAL2043), dorsal vertebra in posterior (E), anterior (F), dorsal (G), and right lateral view (H). **I–L.** KUL-F13 (PAL2046), cervical vertebra in posterior (I), anterior (J), dorsal (K), and right lateral view (L). **M–P.** KUL-F14 (PAL2048), first caudal vertebra in posterior (M), anterior (N), dorsal (O), and right lateral view (P). **Q–T.** KUL-F70, sacral vertebra in posterior (Q), anterior (R), dorsal (S), and right lateral view (T). Provenance: Saint-Gérand-le-Puy. Scale bar = 1 cm.

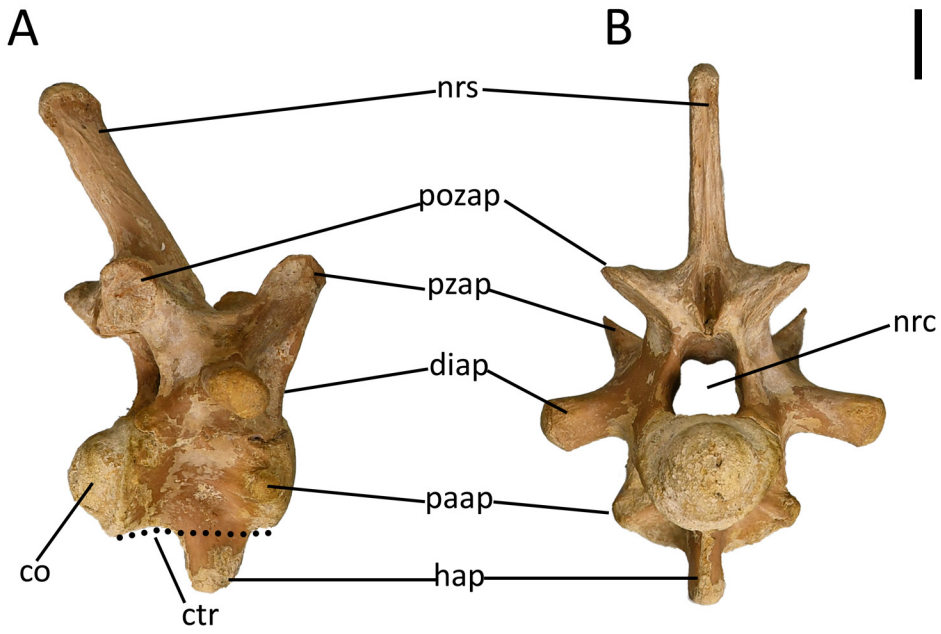

Figure 15. Isolated cervical vertebra of *Diplocynodon ratelii* in right lateral (**A**) and anterior (**B**) view (PLV1983, PAL2046, KUL-F13). Provenance: Saint-Gérand-le-Puy. Scale bar = 1 cm. Anatomical abbreviations: see section 2.5.

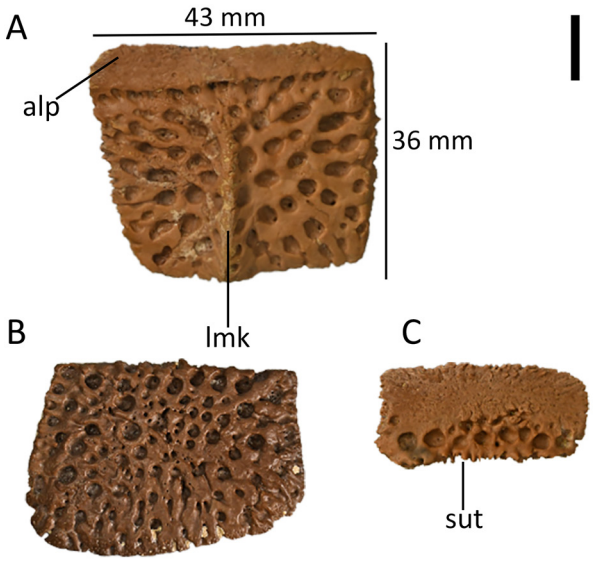

Figure 16. Isolated osteoderms of *Diplocynodon ratelii* (PLV1983, PAL3519). **A.** Dorsal osteoderm in dorsal view (KUL-F22). **B.** Posterior ventral osteoderm in ventral view (KUL-F53). **C.** Anterior ventral osteoderm in ventral view (KUL-F56). Provenance: Saint-Gérand-le-Puy. Scale bar = 1 cm. Anatomical abbreviations: see section 2.5.

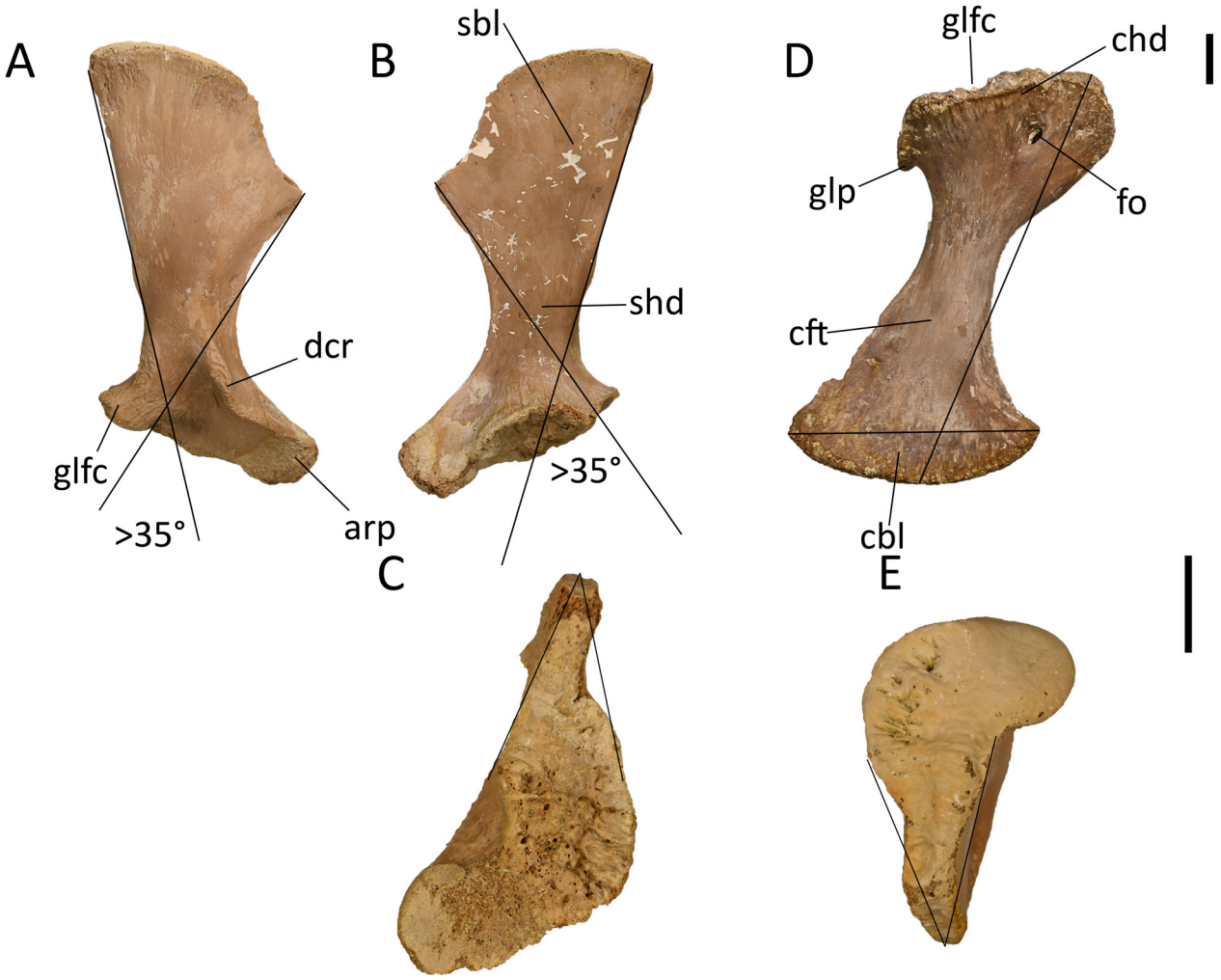

Figure 17. Isolated scapula and coracoid specimens of *Diplocynodon ratelii* (PLV1983). **A–C.** KUL-F8 (PAL2050), right scapula in lateral (A), medial (B), and ventral view (C). **D–E.** KUL-F3 (PAL3450), left coracoid in ventral (D), and dorsal view (E). Provenance: Saint-Gérand-le-Puy. Scale bars = 1 cm; A, B, D use the top scale bar; C, E bottom scale bar. Anatomical abbreviations: see section 2.5.

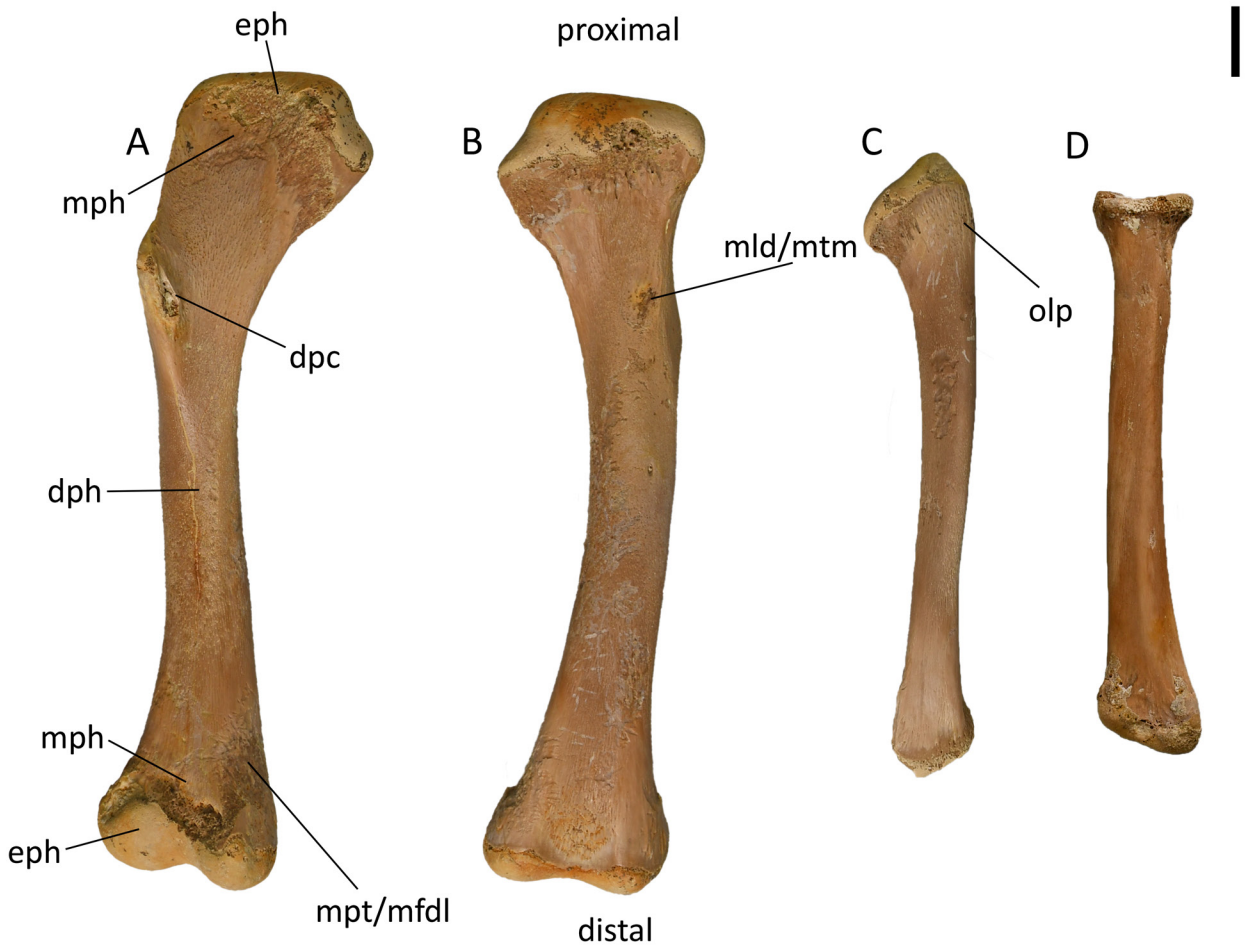

Figure 18. Isolated forelimb specimens of *Diplocynodon ratelii* (PLV1983). **A–B.** KUL-F24 (PAL3597) right humerus in medial (A) and lateral (B) view. **C.** Left ulna (PAL3509, KUL-F32) in lateral view. **D.** Left radius in anterior view (PAL3509, KUL-F34). Provenance: Saint-Gérand-le-Puy. Scale bar = 1 cm. Anatomical abbreviations: see section 2.5.

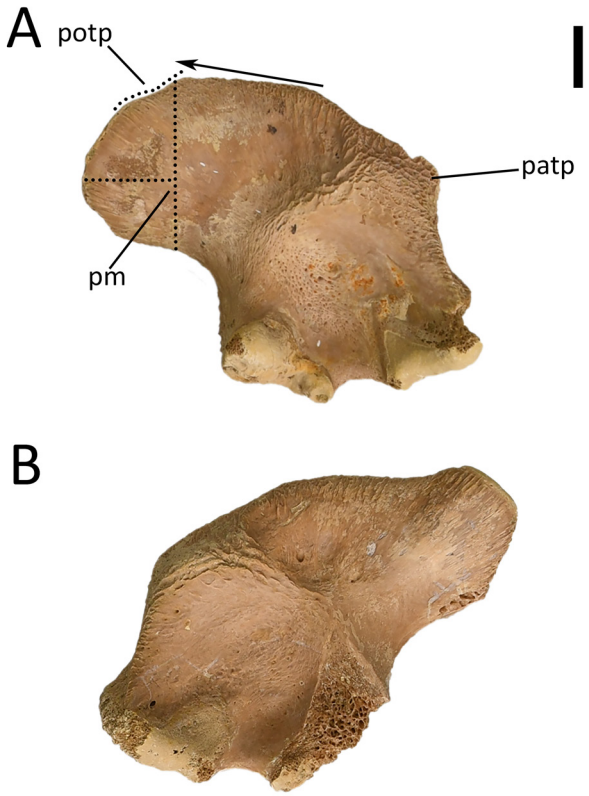

Figure 19. Isolated ilium specimens of *Diplocynodon ratelii* in lateral view (PLV1983). **A.** Right ilium representative for the collection (KUL-F6A). **B.** Left ilium that lacks the deep iliac posterior tip of the iliac blade (KUL-F6B). Provenance: Saint-Gérand-le-Puy. Scale bar = 1 cm. Anatomical abbreviations: see section 2.5.

The postacetabular process projects posteriorly. The condyles are largely symmetric and approximately of equal size. Ilium KUL-F6B (Fig. 19B) is different from the other two in the collection, lacking the deep posterior tip of the iliac blade, exhibiting a shallow morphology instead.

3.2.16. Pubis

The pubis is tilted proximodistally (Fig. 20A). The distal blade gradually widens and does not reach the proximodistal extent. The peduncle is slightly wider than the shaft.

3.2.17. Ischium

Five ischia were recovered from the collection. The ratio of maximum expansion of distal ischial blade to maximum proximodistal length of ischium is 0.527, indicating an intermediate flare of the ischial blade (Fig. 20B).

3.2.18. Femur

Ten femora were recovered from the collection. These are generally longer than humeri. The proximal epiphysis only has one process ventrally and it broadens medially (Fig. 20C). The outline of the proximal epiphysis is convex. There is one prominent muscle scar on the dorsomedial surface of the diaphysis. The bone is slightly sigmoidal in outline and shows a slightly medial bulge in the middle before it strongly curves ventrolaterally more distally. The distal epiphysis is strongly compressed in the middle, and both lobes are approximately equal in size, although the medial lobe projects far more ventrally and is more acute in shape. The fourth trochanter scarring has a very prominent longitudinal ridge on the ventral surface, and there is a rather shallow but large depression immediately medially to the longitudinal ridge.

3.2.19. Fibula

The fibula has a small degree of torsion (Fig. 21A–B). Proximally, the posterior side of the epiphysis is larger, distally, the anterior side is larger. On the proximolateral surface near the anterior edge, there is a trochanter for the insertion of *Musculus iliofibularis*. On the proximomedial surface, there is a smooth triangular crest.

3.2.20. Metacarpals/metatarsals

The metacarpals and metatarsals show different morphologies with some examples shown in Figure 21C–F. Generally, they are all long and thin with a slightly dorsoventrally flattened morphology. The proximal condyle is wider than the distal end with the distal condyle flaring out and flattening.

3.2.21. Phalanges

The phalanges found have a variable morphology with some examples shown in Figure 22A–B, E–F. They are longer than they are wide, with the distal condyle rounded and with a V-shape. The proximal condyle is different between the morphologies with KUL-F27A showing a wide almost triangular proximal condyle and KUL-F27C having a flat condyle that is wider and larger.

3.2.22. Radiale+intermedium

The radiale+intermedium found is short and broad, around twice as long as it is wide (Fig. 22C–D). The distal end is flat while the proximal end is hooked and larger than the distal end. The bone has a slightly flattened morphology, it is not round in cross section.

3.2.23. Ribs

No ribs that are attached to vertebrae have been found. Various morphologies can be found dependent on their position in the

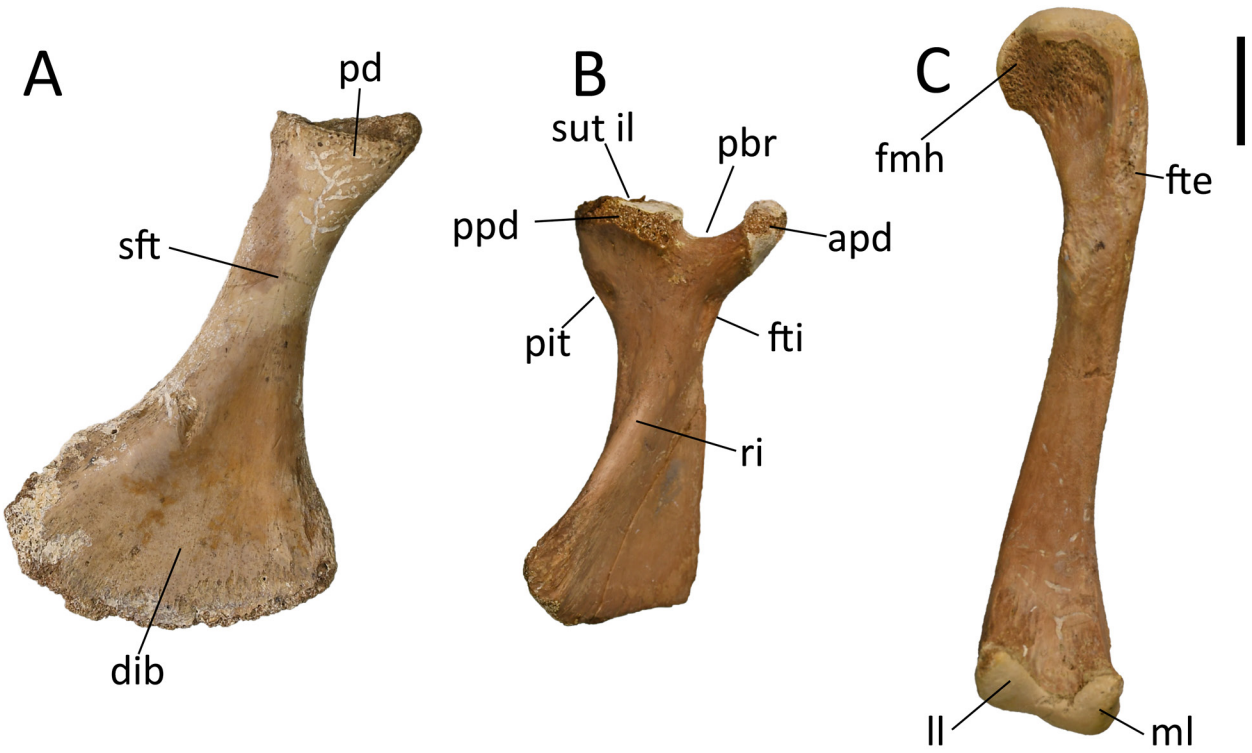

Figure 20. Isolated pubis, ischium and femur specimens of *Diplocynodon ratelii* (PLV1983). **A.** Left pubis in anterolateral view (PAL3450, KUL-F1). **B.** Right ischium in lateral view (KUL-F2). **C.** Right femur in posterior view (PAL3517, KUL-F23). Provenance: Saint-Gérand-le-Puy. Scale bar = 2 cm. Anatomical abbreviations: see section 2.5.

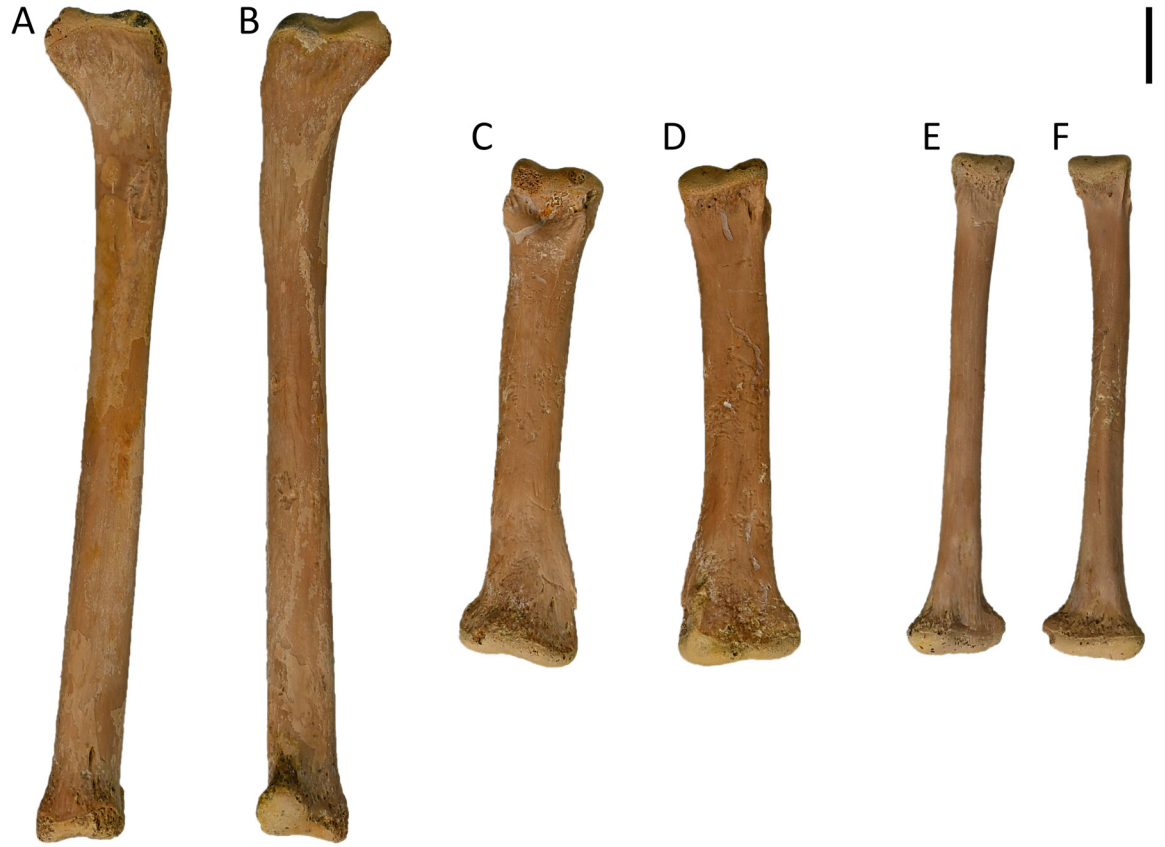

Figure 21. Isolated fibula and metacarpal/metatarsal specimens of *Diplocynodon ratelii* (PLV1983, PAL3509). **A.** Right fibula in lateral view (KUL-F36). **B.** Right fibula in medial view. **C–D.** KUL-F35, metacarpal/metatarsal. **E–F.** KUL-F41, metacarpal/metatarsal. Provenance: Saint-Gérand-le-Puy. Scale bar = 1 cm.

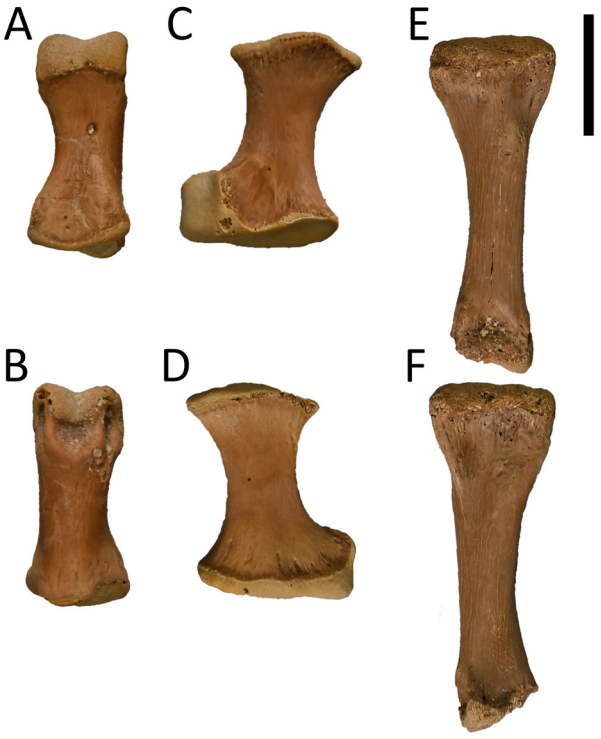

Figure 22. Isolated phalanges and radiale+intermedium specimens of *Diplocynodon ratelii* (PLV1983, PAL3509). **A–B.** KUL-F27A, phalange. **C–D.** KUL-F27B, radiale+intermedium. **E–F.** KUL-F27C, phalange. Provenance: Saint-Gérand-le-Puy. Scale bar = 1 cm.

body (Fig. 23). All ribs have a slightly flat lateral surface, and are generally thin mediolaterally and curved posteriorly.

3.3. Description of selected specimens of Ronzon

In the marl blocks of Ronzon, fragments of cranial structures, axial structures and the appendicular skeleton are present (Figs 24–34). The cranial structures include parts of the frontal, nasal, orbits, postorbitals, supratemporal fenestra and a jugal (Fig. 24). The supratemporal fenestra ends in a sharp point anteriorly. Parts of the postorbitals are present on two different marl blocks (Fig. 26). Additionally, parts of the mandibula and maxilla with teeth are preserved (Fig. 29). Several vertebrae are exposed, one of which is a sacral vertebra (Fig. 27). The block with the sacral vertebra also contains two femora, a fibula, an ilium, and more large bone fragments, almost the whole hip girdle. Other than that, osteoderms, a metacarpal or metatarsal, femora, an ilium, a coracoid, a radius and a fibula are preserved (Fig. 31). In one of the marl blocks, a distinct black piece of rock is present alongside the skeleton (Fig. 25).

4. Discussion

4.1. Relevance

The material of the Filhol collection has been collected in the 19th century but has remained largely undescribed. Given that most specimens in this collection have not been stratigraphically dated and have lost information about their original context or locality, it is conceivable that potentially relevant pieces,

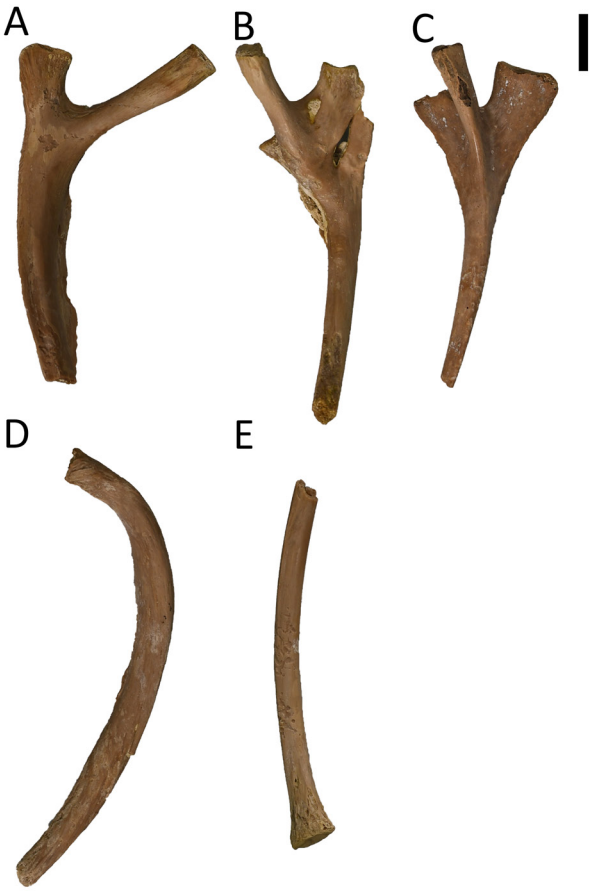

Figure 23. Isolated rib specimens of *Diplocynodon ratelii* (PLV1983, PAL3515). **A.** Dorsal view (KUL-F16A). **B.** Dorsal view (KUL-F16B). **C.** Dorsal view (KUL-F16C). **D.** Lateral view (KUL-F17A). **E.** Lateral view (KUL-F17B). Provenance: Saint-Gérand-le-Puy. Scale bar = 1 cm.

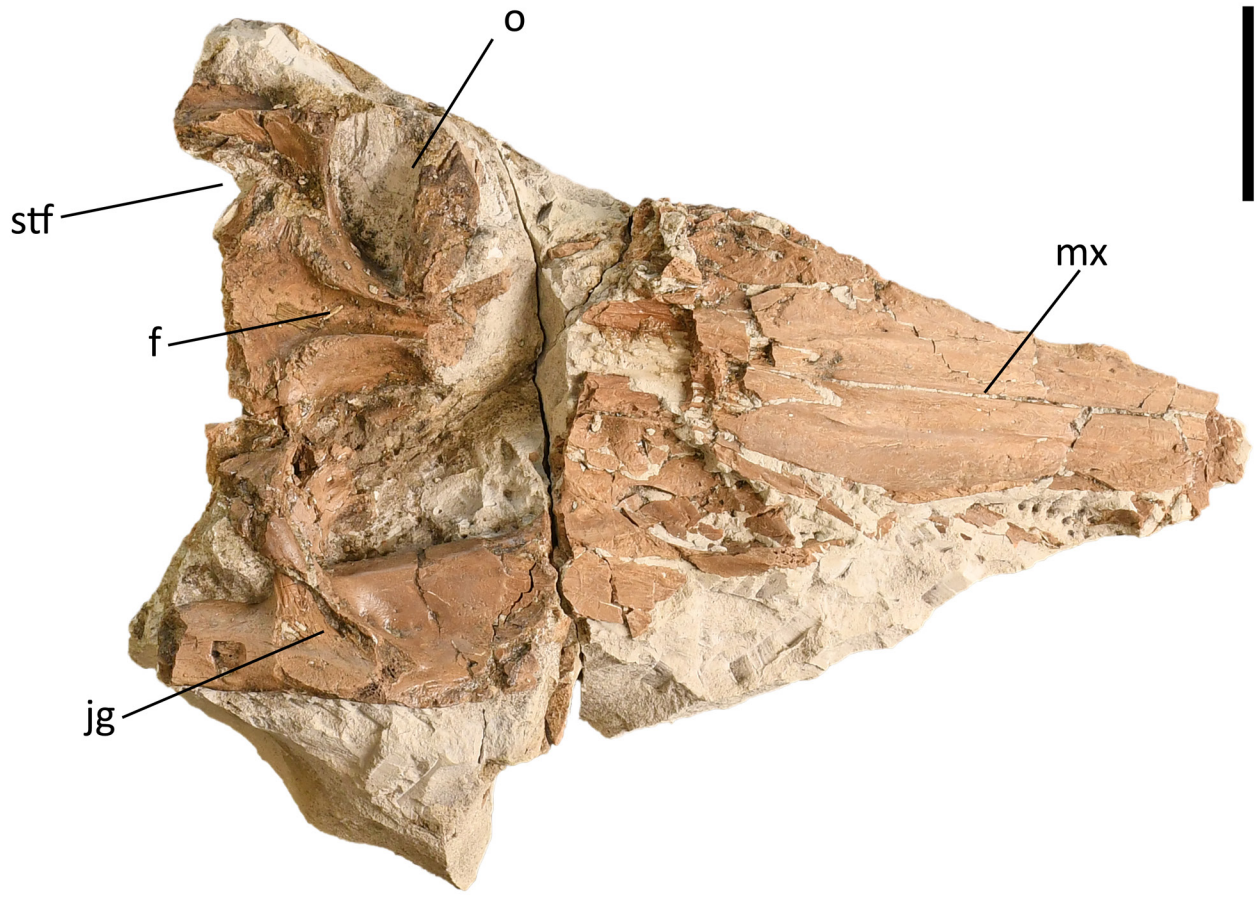

Figure 24. Frontal, maxilla, orbits, part of the supratemporal fenestrae and a jugal of Crocodylia indet. (KUL-F64) in ventral view. Provenance: Ronzon. Scale bar = 3 cm. Anatomical abbreviations: see section 2.5.

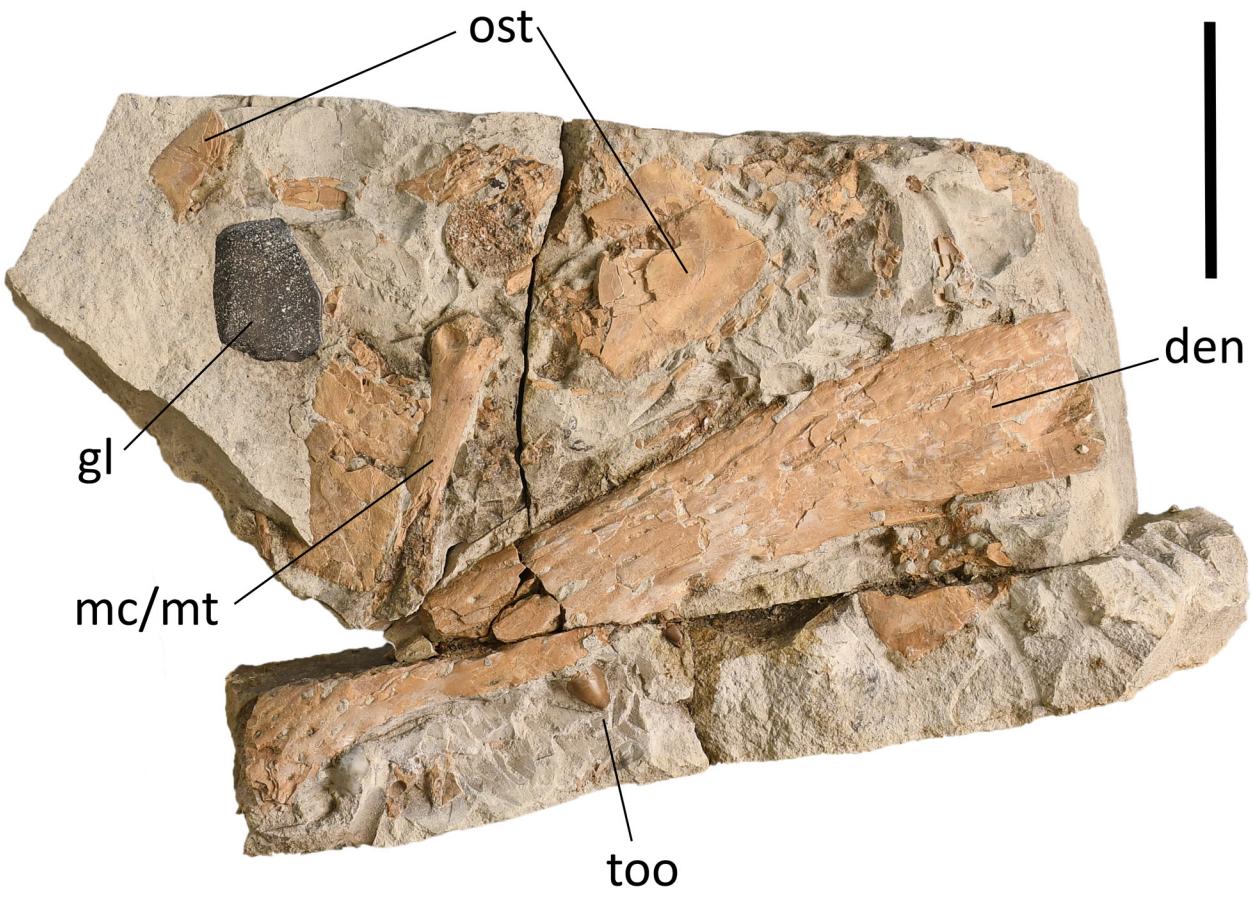

Figure 25. Ventral view of osteoderms, right lateral view of mandibula/maxilla with teeth, a cross section of a bone of the appendicular skeleton, a metacarpal/metatarsal and a gastrolith of Crocodylia indet. (KUL-F59). Provenance: Ronzon. Scale bar = 5 cm. Anatomical abbreviations: see section 2.5.

Figure 26. A ventral view of the postorbital of Crocodylia indet. (KUL-F67). Provenance: Ronzon. Scale bar = 2 cm.

e.g. remains from the same individual, have been moved or lost. Such loss has previously occurred with the holotype of the lizard *Pseudeumeces cadurcensis*, originally described by Filhol and issued from Quercy (Bolet et al., 2017), an example that mirrors the history of the KU Leuven Filhol collection. The fossil material present in the collection consists of around 800 specimens, which is considerable in number. The number of fragments and well-preserved *Diplocynodon* bones in the Filhol collection exceeds the amount of material used or described in many other studies (e.g. Martin, 2010; Luján et al., 2019; Chroust et al., 2021). Moreover, the diversity of bone elements (and their disarticulated state) provides a good representation of the complete anatomy including views of the endocranial anatomy of this taxon (e.g. Figs 3, 4, 13). The use of fossil collections to advance our knowledge on the morphology, distribution, ecology and evolution of crocodylians highlights the value of maintaining fossil collections and making them accessible. Inventorying and publishing existing collections can improve previous descriptional or phylogenetic work (e.g. Walter et al., 2026) but may also aid palaeohistological studies, for which a large sample of taxonomically identified bones is often needed (e.g. Hoffman et al., 2025). Additionally, it prevents the collection from fading into obscurity, ensuring it is not overlooked from both a scientific research and cultural heritage perspective. Crocodylian palaeontology is an active field of research where uncertainties in classification remain (e.g. Rio & Mannion, 2021; Massonne & Böhme, 2022; Ruebenstahl et al., 2022).

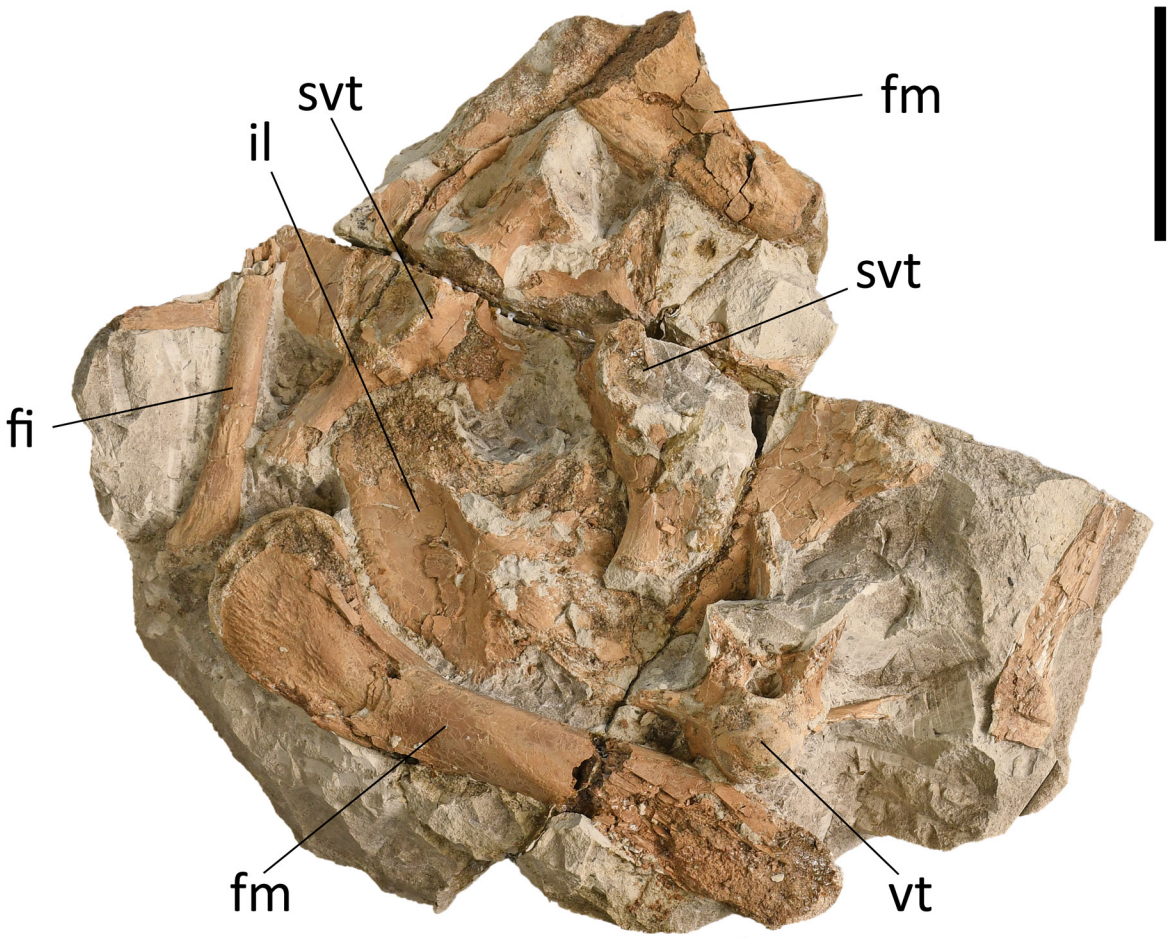

Figure 27. A lateral view of two femora and ilium, an anterior view of a vertebra, two sacral vertebrae and a fibula of Crocodylia indet. (KUL-F61). Provenance: Ronzon. Scale bar = 5 cm. Anatomical abbreviations: see section 2.5.

Figure 28. A lateral view of part of a maxilla/premaxilla of Crocodylia indet. (KUL-F68). Provenance: Ronzon. Scale bar = 2 cm.

Figure 29. Right lateral view of part of a dentary/maxilla of Crocodylia indet. (KUL-F66). Provenance: Ronzon. Scale bar = 2 cm.

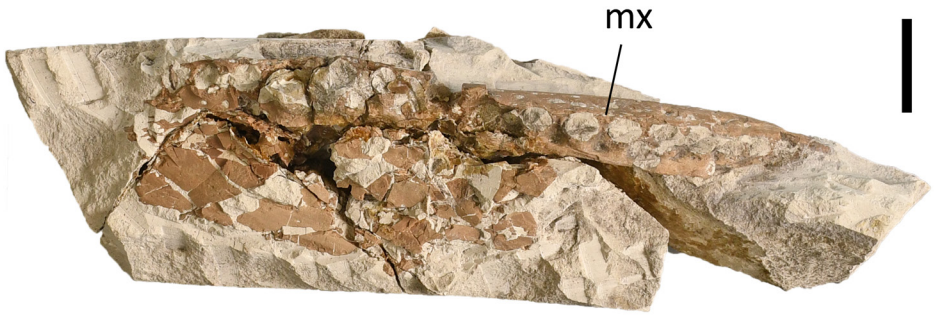

Figure 30. A ventral view of a maxilla of Crocodylia indet. (KUL-F62). Provenance: Ronzon. Scale bar = 2 cm. Anatomical abbreviation: see section 2.5.

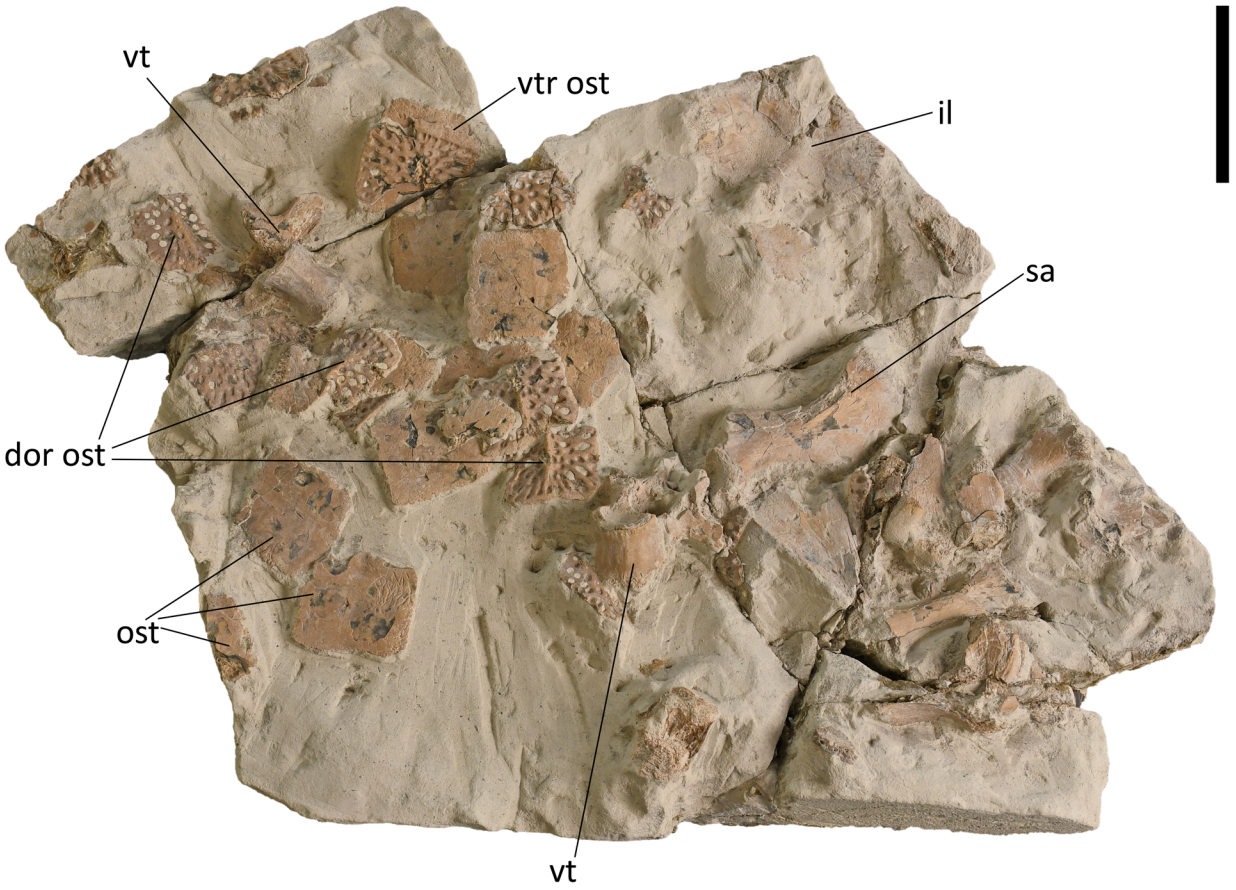

Figure 31. Ventral and dorsal view of osteoderms, a posterior view of a vertebra and a lateral view of a scapula, ilium and other bone fragments of Crocodylia indet. (KUL-F63). Provenance: Ronzon. Scale bar = 5 cm. Anatomical abbreviations: see section 2.5.

4.2. Saint-Gérand-le-Puy

The crocodylian material from Saint-Gérand-le-Puy exhibited several morphologies that together are found in *Diplocynodon*. Two subequal alveoli in the maxilla and subequal, confluent alveoli in the dentary, are visible on specimens KUL-F49, KUL-F48, KUL-F44, KUL-F42 (Fig. 7C, D; Fig. 8A, B; Díaz Aráez et al., 2017; Luján et al., 2019; Massonne & Böhme, 2022; Walter, 2025). A foramen aëreum far from the medial edge of the quadrate and a small, ventrally reflected medial hemicondyle of the quadrate (Díaz Aráez et al., 2017; Luján et al., 2019) are also present in the collection on specimen KUL-F7 (Fig. 6). Keeled dorsal osteoderms and bipartite ventral osteoderms (Díaz Aráez et al., 2017; Massonne & Böhme, 2022; Walter, 2025) are shown in Figure 16 on specimens KUL-F22, KUL-F53 and KUL-F56. Specimen KUL-F6A clearly shows the rounded dorsal margin of the ilium and the deep posterior tip of the iliac blade mentioned by Massonne & Böhme (2022) and Walter (2025) (Fig. 19). The frontoparietal suture as seen on specimen KUL-F4 is not linear (Fig. 2D). Although most *Diplocynodon* species have a linear frontoparietal suture and this has been mentioned as a character of *Diplocynodon* (Massonne & Böhme, 2022), some species such as *Diplocynodon ratelii* have a non-linear frontoparietal suture (Díaz Aráez et al., 2017). The combination of these characters makes it possible to assign the specimens to *Diplocynodon*.

To diagnose to species level, characters differing within *Diplocynodon* were used. Luján et al. (2019) named the shape

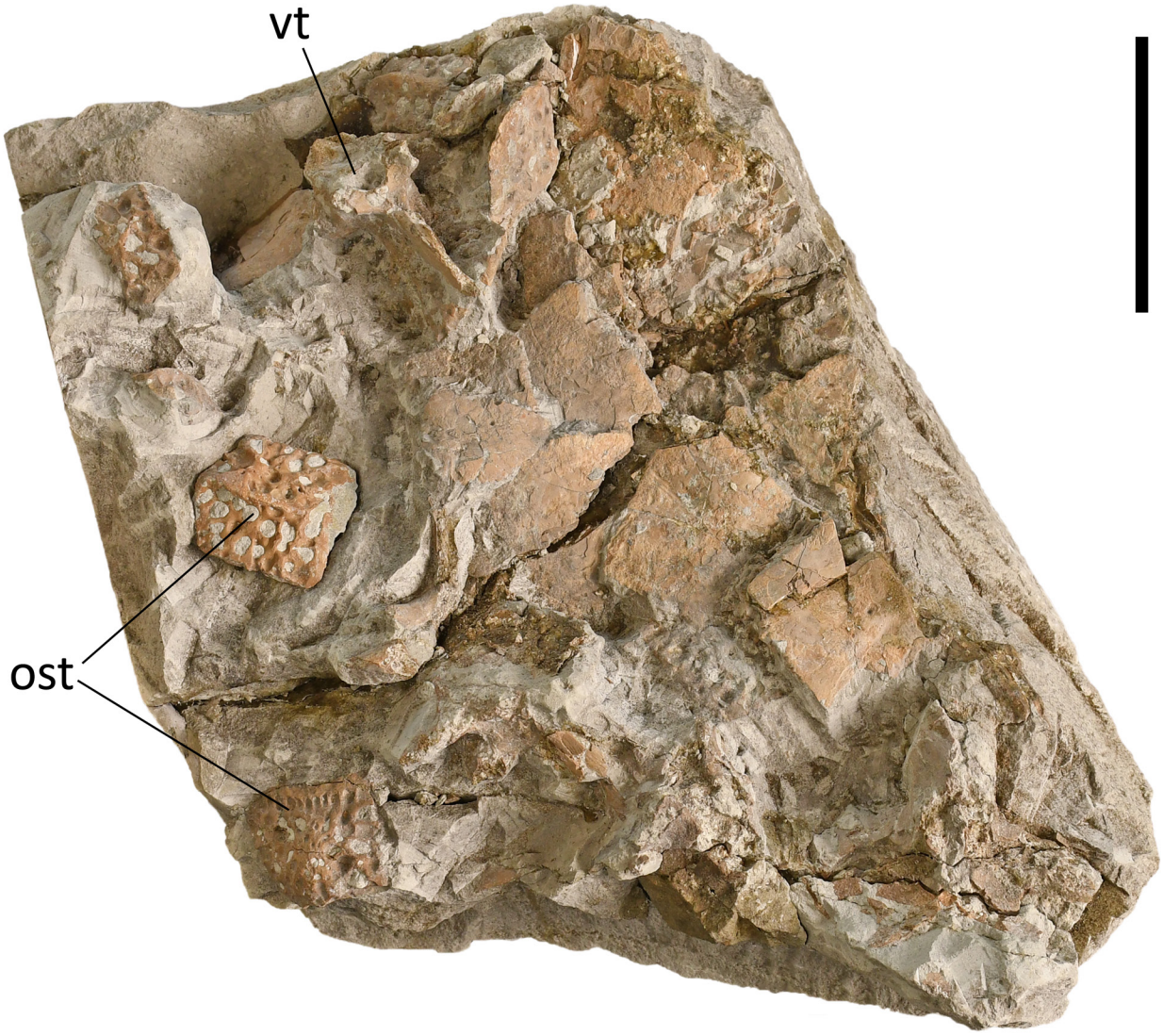

Figure 32. Dorsal view of osteoderms, a posterior view of a vertebra and many bone fragments of Crocodylia indet. (KUL-F60). Provenance: Ronzon. Scale bar = 5 cm. Anatomical abbreviations: see section 2.5.

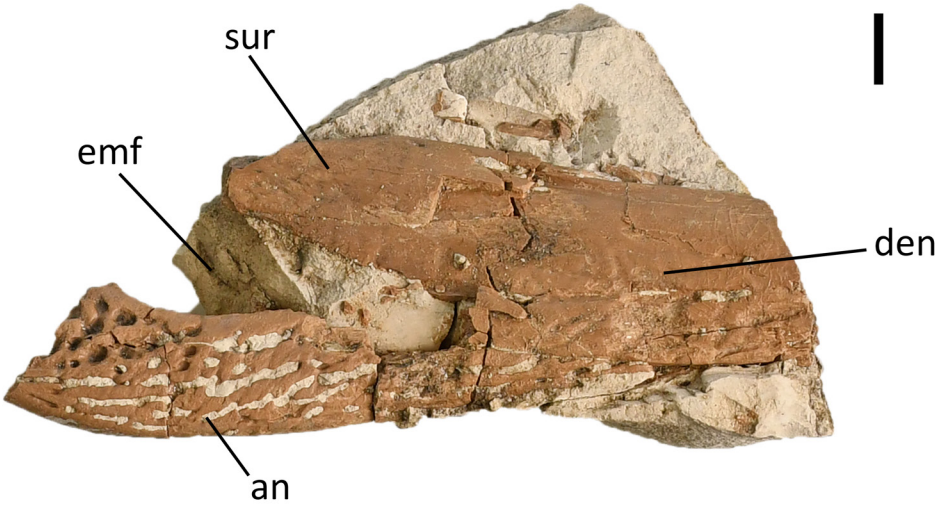

Figure 33. Right lateral view of parts of the angular, dentary and surangular of Crocodylia indet. (KUL-F65). Provenance: Ronzon. Scale bar = 1 cm. Anatomical abbreviations: see section 2.5.

Figure 34. Ventral view of maxilla(e) and a long bone of Crocodylia indet. (KUL-F69). Provenance: Ronzon. Scale bar = 5 cm. Anatomical abbreviations: see section 2.5.

of the modestly posteriorly convex fronto-parietal suture, the contour of the naris (a crest-like thickening surrounding the external naris), the extension of the dentary symphysis (reaching the posterior margin of the fourth alveolus) as diagnostic features of *Diplocynodon ratelii*. These characters are preserved on specimens KUL-F4, KUL-F31 and KUL-F44 (Fig. 2D; Fig. 7A; Fig. 8A). Only *D. ratelii*, *D. muelleri* and *D. remensis* have a short symphysis reaching the fourth to fifth alveolus (Brochu et al., 2012; Martin et al., 2014; Díaz Aráez et al., 2017). Furthermore, only *D. ratelii* and *D. ungeri* possess a modestly posteriorly convex frontoparietal suture and only *D. ratelii* and *D. muelleri* possess the crest around the naris (Brochu et al., 2012; Martin et al., 2014; Díaz Aráez et al., 2017). The frontoparietal suture has not been preserved in *D. elavericus* and it has a thickened crest around the naris but it does not have a short symphysis, so this species can be excluded (Díaz Aráez et al., 2017). This combination of features makes it possible to refer the remains from Saint-Gérand-le-Puy in the KU Leuven Filhol collection to the species *Diplocynodon ratelii*, confirming the previous, preliminary diagnosis. While this identification cannot be confirmed with the new diagnostic key by Walter (2025), as that used characters which require articulated specimens, the identification as *D. ratelii* here is in accordance with the earlier finds in the region (Pomel, 1847; Vaillant, 1872; Berg, 1966; Martin, 2010).

Nevertheless, it remains possible that not all remains belong to the same species. For example, the collection also comprises a typical crocodylian ilium (KUL-F6B) that lacks the deep iliac posterior tip of the iliac blade diagnostic of *Diplocynodon* (Rio et al., 2020) (Fig. 19). This could suggest that a different crocodylian genus occurred at Saint-Gérand-le-Puy. However, at the moment little is known about morphological variability within *D. ratelii*, especially from the postcranial skeleton. Therefore, it might be that the encountered ilium reflects morphological variability within the species *D. ratelii*. Another possibility is that deformation during fossilisation changed the shape of this ilium and *D. ratelii* still is the only species present at this locality.

4.3. Ronzon

The fossil material from Ronzon dates from the early Oligocene. From the genus *Diplocynodon*, only the species *D. muelleri* and *D. "gervaisi"* are known from this time period. *Diplocynodon "gervaisi"* was first recovered from Ronzon (Gervais, 1859; Berg, 1966), which makes it a likely candidate for identification.

While *D. "gervaisi"* is the only known species of Crocodylia from Ronzon, it is currently not an accepted species (Martin, 2010; Venczel, 2023). The fossil record of *D. "gervaisi"* is very poor and is in need of reappraisal (Massonne & Böhme, 2022; Walter, 2025).

The characteristics of *Diplocynodon "gervaisi"* listed by Berg (1966) are for the most part not visible on the specimens present in the Filhol collection. This makes it impossible to compare the remains to the ones described earlier of *Diplocynodon "gervaisi"*. All defined characteristics of this species are restricted to the skull, primarily on the mandible and maxilla (Berg, 1966). These characteristics are not visible in the specimens present in the Filhol collection, as the bones are embedded in a marl matrix that blocks the view. Only one character is partly visible, the pointed shape of the supratemporal fenestrae, which is visible on the posterior side of specimen KUL-F64 (Fig. 24; Berg, 1966). However, the pointed shape of the supratemporal fenestrae could also be a sign of a juvenile instead of being comparable to *D. "gervaisi"* (Cossette et al., 2022). The only other characteristics mentioned about *D. "gervaisi"* are the skull length, skull width/length ratio and dental formulas (Berg, 1966). However, even the most complete part of the skull present in the collection is not sufficiently complete to measure the length of the skull.

While it is possible that the specimens from Ronzon are from a different species than *Diplocynodon "gervaisi"*, this is also difficult to determine. None of the characteristics widely used to define *Diplocynodon* are visible in the collection (Díaz Aráez et al., 2017; Massonne & Böhme, 2022). Neither the third nor the fourth dentary alveoli are visible, nor are there any osteoderms preserved in the correct position (Díaz Aráez et al., 2017; Massonne & Böhme, 2022). Additionally, the frontoparietal suture is fragmented (Fig. 24), and the quadrate was not present or hidden in the matrix (Díaz Aráez et al., 2017; Massonne & Böhme, 2022). The frontal is only visible from the underside (Fig. 24), and the ilium is fragmented (Fig. 27). Therefore, the material from Ronzon cannot be assigned to a genus or species unless more or better characteristics are found, more parts of the specimens are uncovered and/or *Diplocynodon "gervaisi"* is revised. But because the overall shape of the bones present in the collection does not differ from known *Diplocynodon* bones and *Diplocynodon* sp. is known from Ronzon in collections from the Natural History Museum in Basel (NMB), Switzerland, it is highly likely that all specimens from Ronzon come from *Diplocynodon* sp. The material from Ronzon from the Filhol collection can possibly be used in the future to revise *D. "gervaisi"* if compared first hand with known material from *D. "gervaisi"* from other collections (e.g. NMB, Basel, Switzerland) or by using techniques like CT-scanning to reveal the bones inside the marl.

4.4. Full collection

This study contributes to the known specimens from Saint-Gérand-le-Puy and Ronzon. The minimal number of individuals present in the collection from Saint-Gérand-le-Puy can be determined by assessing the number of single or pairwise bone fragments (Table 2). As there are 18 ectopterygoids (the most common pairwise bone found in the collection), seven right elements and seven left elements with the other four unidentifiable left or right. As at least two of the unidentifiable elements must come from the same side, the material comes from at least nine individuals. There is a high chance that the material from Ronzon comes from at least two individuals because specimens KUL-F64 and KUL-F67 visible in Figures 24 and 26 both show surroundings of the orbital in a way that is not compatible with each other.

Having more available specimens can help with future research on those localities or on the species represented in this collection. Especially the materials from Ronzon can aid in the knowledge on *Diplocynodon*, because the *Diplocynodon* material from Ronzon is currently not assigned to a species. Moreover, this material presents potential evidence for the presence of gastroliths in *Diplocynodon*. KUL-F59 shows a large black stone, of approximately 2.5 cm in diameter, with rounded edges, that contrasts with the fine-grained sedimentary matrix in which it sits (Fig. 25). The fine-grained sediments of the Ronzon material suggest that it is unlikely that this stone was transported by high-energy sedimentary processes. Instead, it has previously been established that the Eocene *Diplocynodon deponiae* bore gastroliths (Delfino & Smith, 2012). Therefore, we consider it likely that the stone recorded here is also a gastrolith, indicating that the bearing of gastroliths was a more common practice among *Diplocynodon* species.

To conclude, the crocodylian remains of the Filhol collection at KU Leuven consist of around 800 remains from Saint-Gérand-le-Puy and 11 marl tablets and some fragments from Ronzon. The remains from Saint-Gérand-le-Puy contain collectively enough characteristics to be attributed to *Diplocynodon ratelii*. It is currently not possible to attribute the specimens from Ronzon to a species, but it is likely that the specimens are from *Diplocynodon* sp. The remains from Ronzon are subjects for future research. The full Filhol collection of the KU Leuven can be used for future research on fossil Crocodylia from France. This collection can now be viewed using the photographs and list of all specimens.

5. Future research

Some questions arise from this study, e.g. whether the remains from Ronzon can be attributed to *Diplocynodon "gervaisi"* and if *D. "gervaisi"* is a valid species. The *Diplocynodon* remains from Ronzon, embedded in marl, still have to be determined. The presence of skull, osteoderm and appendicular fragments allows for a meaningful determination of the remains. However, using non-destructive scanning techniques could be necessary to reveal characteristics that are currently hidden by the sedimentary matrix.

In recent research, the focus is often on cranial morphology and characteristics. Further expanding on characteristics from the appendicular skeleton might reveal additional autapomorphies that would aid in resolving relationships within the genus *Diplocynodon*. Additionally, the remains from Ronzon contain more appendicular fragments which might provide further insights into *D. "gervaisi"* which has very limited descriptions.

A second critical question is whether the aberrant ilium belongs to *Diplocynodon ratelii* or if it belongs to a second species. Statistical comparisons between ilia from *D. ratelii* in other palaeontological collections could be done to investigate the morphological variation within the species *D. ratelii*. Reevaluating existing collections for future research provides the potential to add significant new insights into crocodylian palaeontological research.

Author contributions

Sophie Boerman and Johan Vellekoop conceptualized this research. Anne Basten, Pascal van der Bij, and Wouter Berings performed this study as a part of their BSc thesis in Biology

at KU Leuven. All three conducted literature reviews and co-wrote the manuscript. Practical tasks such as sorting, cleaning, photographing, and editing specimens were shared, with Anne Basten specializing in repairs while Wouter Berings and Pascal van der Bij specialized in photography. All five authors aided in the diagnoses of the specimens, discussed results and reviewed the manuscript text. Anne Basten put her main focus on introduction and discussion, while Pascal van der Bij put his main focus on results and figures.

Acknowledgements

This work was funded by the Belgian Science Policy Office (BELSPO) through FED-tWIN project Prf-2020-038 (MicroPAST) and by the Fonds Wetenschappelijk Onderzoek (FWO) grant 11PM124N (to SB). We thank Torsten Scheyer (University of Zurich) and Jules D. Walter (Università degli Studi di Torino, and Eberhard Karls Universität Tübingen) for their helpful comments on our manuscript in the review process.

References

Anonymous, 1902. Dr. Henri Filhol. Nature, 66(1701), 133–134. https://doi.org/10.1038/066133a0

Benton, M.J. & Clark, J.M., 1988. Archosaur phylogeny and the relationships of the Crocodylia. In Benton, M.J. (ed.), The Phylogeny and Classification of the Tetrapods. Volume 1: Amphibians, Reptiles, Birds. Clarendon Press, Oxford, 295–338.

Berg, D.E., 1966. Die Krokodile, insbesondere *Asiatosuchus* und aff. *Sebecus*?, aus dem Eozän von Messel bei Darmstadt/Hessen. Abhandlung des Hessischen Landesamtes für Bodenforschung, 52, 3–105.

Bolet, A., Rage, J.C. & Conrad, J.L., 2017. Rediscovery of the long-lost holotype of the lacertid lizard *Pseudeumeces cadurcensis* (Filhol, 1877). Journal of Vertebrate Paleontology, 37(3), e1315669. https://doi.org/10.1080/02724634.2017.1315669

Brochu, C.A., 1999. Phylogenetics, taxonomy, and historical biogeography of alligatoroidea. Journal of Vertebrate Paleontology, 19(supp002), 9–100. https://doi.org/10.1080/02724634.1999.10011201

Brochu, C.A., 2003. Phylogenetic approaches toward crocodylian history. Annual Review of Earth and Planetary Sciences, 31, 357–397 https://doi.org/10.1146/annurev.earth.31.100901.141308

Brochu, C.A., Parris, D.C., Grandstaff, B.S., Denton, R.K. & Gallagher, W.B., 2012. A new species of *Borealosuchus* (Crocodyliformes, Eusuchia) from the Late Cretaceous–early Paleogene of New Jersey. Journal of Vertebrate Paleontology, 32(1), 105–116. https://doi.org/10.1080/02724634.2012.633585

Bucher, H., Ginsburg, L. & Cheneval, J., 1985. Nouvelles données et interprétations sur la formation des gisements de vertébrés aquitaniens de Saint-Gérand-le-Puy (Allier, France). Geobios, 18(6), 823–832. https://doi.org/10.1016/S0016-6995(85)80037-1

Buscalioni, A.D., Sanz, J.L. & Casanovas, M.L., 1992. A new species of the eusuchian crocodile *Diplocynodon* from the Eocene of Spain. Neues Jahrbuch für Geologie und Paläontologie, Abhandlungen, 187, 1–29. https://doi.org/10.1127/njgpa/187/1992/1

Cheneval, J., 1989. Fossil bird study, and paleoecological and paleoenvironmental consequences: Example from the Saint-Gérand-le-Puy deposits (lower Miocene, Allier, France). Palaeogeography, Palaeoclimatology, Palaeoecology, 73(3-4), 295–309. https://doi.org/10.1016/0031-0182(89)90010-2

Chroust, M., Mazuch, M., Ivanov, M., Ekrt, B. & Luján, À.H., 2021. First remains of *Diplocynodon* cf. *ratelii* from the early Miocene sites of Ahníkov (Most Basin, Czech Republic). Bulletin of Geosciences, 96(2), 123–138. https://doi.org/10.3140/bull.geosci.1803

Cossette, A.P., Grass, A.D. & DeGuzman, T., 2022. The contribution of ontogenetic growth trajectories on the divergent evolution of the crocodylian skull table. The Anatomical Record, 305(10), 2904–2925. https://doi.org/10.1002/ar.24824

Darlim, G., Lee, M.S.Y., Walter, J. & Rabi, M., 2022. The impact of molecular data on the phylogenetic position of the putative oldest crown crocodilian and the age of the clade. Biology Letters, 18(2), 20210603. https://doi.org/10.1098/rsbl.2021.0603

Delfino, M. & Smith, T., 2012. Reappraisal of the morphology and phylogenetic relationships of the middle Eocene alligatoroid *Diplocynodon deponiae* (Frey, Laemmert, and Riess, 1987) based on a three-dimensional specimen. Journal of Vertebrate Paleontology, 32(6), 1358–1369. https://doi.org/10.1080/02724634.2012.699484

Delfino, M., Böhme, M. & Rook, L., 2007. First European evidence for transcontinental dispersal of *Crocodylus* (late Neogene of southern Italy). Zoological Journal of the Linnean Society, 149(3), 293–307. https://doi.org/10.1111/j.1096-3642.2007.00248.x

Díaz Aráez, J.L., Delfino, M., Luján, À.H., Fortuny, J., Bernardini, F. & Alba, D.M., 2017. New remains of *Diplocynodon* (Crocodylia: Diplocynodontidae) from the Early Miocene of the Iberian Peninsula. Comptes Rendus Palevol, 16(1), 12–26. https://doi.org/10.1016/j.crpv.2015.11.003

Efimov, M.B., 1988. The fossil crocodiles and champsosaurides of Mongolia and the USSR. Transactions of the Joint Soviet–Mongolian Palaeontological Expedition, 36, 1–108. [In Russian].

Filhol, H., 1876/1877. Recherches sur les phosphorites du Quercy. Annales des Sciences géologiques, 7-8, 1–558.

Filhol, H., 1879/1880. Étude des mammifères fossiles de Saint-Gérand-le-Puy (Allier). Annales des Sciences géologiques, 10, 1–252 & 11, 1–86.

Filhol, H., 1881. Étude des mammifères fossiles de Ronzon (Haute-Loire). Annales des Sciences géologiques, 12, 1–270.

Filhol, H., 1883. Note sur quelques mammifères fossiles de l'époque miocène. Archives du Museum d'histoire naturelle de Lyon, 3, 1–99. https://doi.org/10.3406/mhnly.1883.940

Fournier, M., Ladevèze, S., Le Verger, K., Fischer, V., Speijer, R.P. & Solé, F., 2020. On the morphology of the astragalus and calcaneus of the amphicyonids (Carnivora, Mammalia) from the Paleogene of Europe: implications for the ecology of the European bear-dogs. Geodiversitas, 42(18), 305–325. https://doi.org/10.5252/geodiversitas2020v42a18

Frey, E., Laemmert, A. & Riess, J., 1987. *Baryphracta deponiae* n.g. n.sp. (Reptilia, Crocodylia), ein neues Krokodil aus der Grube Messel bei Darmstadt (Hessen, Bundesrepublik Deutschland). Neues Jahrbuch für Geologie und Paläontologie, Monatshefte, 1987(1), 15–26.

Gervais, P., 1859. Zoologie et paléontologie françaises : nouvelles recherches sur les animaux vertébrés dont on trouve les ossements enfouis dans le sol de la France et sur leur comparaison avec les espèces propres aux autres régions du globe. 2e éd. Arthus Bertrand, Paris, 544 p.

Gmelin, J.F., 1789. Caroli a Linné. Systema naturae per regna tri naturae, secundum classes, ordines, genera, species, cum characteribus, differentiis, synonymis, locis. Tomus 1, pars 3. G.E. Beer, Leipzig, 1033–1516. https://doi.org/10.5962/bhl.title.36932

Göhlich, U.B. & Mourer-Chauviré, C., 2005. Revision of the phasianids (Aves: Galliformes) from the Lower Miocene of Saint-Gérand-le-Puy (Allier, France). Palaeontology, 48(6), 1331–1350. https://doi.org/10.1111/j.1475-4983.2005.00520.x

Górka, M., Březina, J., Chroust, M., Kowalski, R., López-Torres, S. &

Tałanda, M. 2025. Crocodylian remains from the Miocene of the Fore-Carpathian Basin and its foreland—including the world's northernmost Neogene crocodilian. Acta Palaeontologica Polonica 70(2), 225–251. https://doi.org/10.4202/app.01194.2024

Gray, J.E., 1844. Catalogue of the tortoises, crocodiles, and amphisbænians, in the collection of the British Museum. British Museum (Natural History), London, 80 p. https://doi.org/10.5962/bhl.title.5501

Groh, S.S., Upchurch, P., Day, J.J. & Barrett, P.M., 2023. The biogeographic history of neosuchian crocodiles and the impact of saltwater tolerance variability. Royal Society Open Science, 10(10), 230725. https://doi.org/10.1098/rsos.230725

Hastings, A.K. & Hellmund, M., 2015. Rare in situ preservation of adult Crocodylian with eggs from the Middle Eocene of Geiseltal, Germany. Palaios, 30(6), 446–461. https://doi.org/10.2110/palo.2014.062

Hoffman, D.K., Goldsmith, E.R., Houssaye, A., Maidment, S.C.R., Felice, R.N. & Mannion, P.D., 2025. Evolution of growth strategy in alligators and caimans informed by osteohistology of the late Eocene early-diverging alligatoroid crocodylian *Diplocynodon hantoniensis*. Journal of Anatomy, 247(1), 165–178. https://doi.org/10.1111/joa.14231

Huene, F.V. & Nikoloff, I., 1963. Ein pliozänes Krokodil in Bulgarien. Neues Jahrbuch für Geologie und Paläontologie, Abhandlungen, 1963(118), 266–271.

Huxley, T.H., 1875. On *Stagonolepis robertsoni*, and on the evolution of the Crocodilia. Quarterly Journal of the Geological Society 31(1-4), 423–438. https://doi.org/10.1144/GSL.JGS.1875.031.01-04.29

Kälin, J.A., 1936. *Hispanochampsa mülleri* nov. gen. nov. spec., ein neuer Crocodilide aus dem unteren Oligocaen von Tárrega (Catalonien). Abhandlungen der Schweizerischen palaeontologischen Gesellschaft, 58, 1–40.

Kuzmin, I.T. & Zvonok, E.A., 2021. Crocodylian assemblage from the middle Eocene Ikovo locality (Lugansk Province, Ukraine), with a discussion of the fossil record and geographic origins of crocodyliform fauna in the Paleogene of Europe. Geobios, 65, 7–27. https://doi.org/10.1016/j.geobios.2021.02.002

Lange-Badré, B., 1979. Les Créodontes (Mammalia) d'Europe occidentale de l'Éocène supérieur à l'Oligocène supérieur. Mémoires du Muséum national d'Histoire naturelle, Série C, Sciences de la Terre, 42, 1–249.

Lee, M.S.Y. & Yates, A.M., 2018. Tip-dating and homoplasy: reconciling the shallow molecular divergences of modern gharials with their long fossil record. Proceedings of the Royal Society B, 285(1881), 20181071. https://doi.org/10.1098/rspb.2018.1071

Ludwig, R., 1877. Fossile Crocodiliden aus der Tertiärformation des Mainzer Beckens. Palaeontographica, Supplementbände, 3(4-5), 1–52.

Luján, À.H., Chroust, M., Čerňanský, A., Fortuny, J., Mazuch, M. & Ivanov, M., 2019. First record of *Diplocynodon ratelii* Pomel, 1847 from the early Miocene site of Tušimice (Most Basin, Northwest Bohemia, Czech Republic). Comptes Rendus Palevol, 18(7), 877–889. https://doi.org/10.1016/j.crpv.2019.04.002

Macaluso, L., Martin, J.E., Del Favero, L. & Delfino, M., 2019. Revision of the crocodilians from the Oligocene of Monteviale, Italy, and the diversity of European eusuchians across the Eocene-Oligocene Boundary. Journal of Vertebrate Paleontology, 39(2), e1601098. https://doi.org/10.1080/02724634.2019.1601098

Markwick, P.J., 1998. Fossil crocodilians as indicators of Late Cretaceous and Cenozoic climates: implications for using palaeontological data in reconstructing palaeoclimate. Palaeogeography, Palaeoclimatology, Palaeoecology, 137(3-4), 205–271. https://doi.org/10.1016/S0031-0182(97)00108-9

Martin, J.E., 2010. A new species of *Diplocynodon* (Crocodylia, Alligatoroidea) from the Late Eocene of the Massif Central, France, and the evolution of the genus in the climatic context of the Late Palaeogene. Geological Magazine, 147(4), 596–610. https://doi.org/10.1017/S0016756809990161

Martin, J.E. & Gross, M., 2011. Taxonomic clarification of *Diplocynodon* POMEL, 1847 (Crocodilia) from the Miocene of Styria, Austria. Neues Jahrbuch für Geologie und Paläontologie, Abhandlungen, 261(2), 177–193.

Martin, J.E., Smith, T., de Lapparent de Broin, F., Escuillié, F. & Delfino, M., 2014. Late Palaeocene eusuchian remains from Mont de Berru, France, and the origin of the alligatoroid *Diplocynodon*. Zoological Journal of the Linnean Society, 172(4), 867–891. https://doi.org/10.1111/zoj.12195

Martin, S., 2007. Global diversity of crocodiles (Crocodilia, Reptilia) in freshwater. In Balian, E.V., Lévêque, C., Segers, H. & Martens, K. (eds), Freshwater Animal Diversity Assessment. Springer, Dordrecht, Development in Hydrobiology, 198, 587–591. https://doi.org/10.1007/978-1-4020-8259-7_56

Massonne, T. & Böhme, M., 2022. Re-evaluation of the morphology and phylogeny of *Diplocynodon levantinicum* Huene & Nikoloff, 1963 and the stratigraphic age of the West Maritsa coal field (Upper Thrace Basin, Bulgaria). PeerJ, 10, e14167. https://doi.org/10.7717/peerj.14167

Mein, P., 1999. European Miocene mammal biochronology. In Rössner, G.E. & Heissig, K. (eds), The Miocene Land Mammals of Europe. Friedrich Pfeil, München, 25–38.

Mennecart, B., Yerly, B., Mojon, P.-O., Angelone, C., Maridet, O., Böhme, M. & Pirkenseer, C., 2016. A new Late Agenian (MN2a, Early Miocene) fossil assemblage from Wallenried (Molasse Basin, Canton Fribourg, Switzerland). Paläontologische Zeitschrift, 90(1), 101–123. https://doi.org/10.1007/s12542-015-0275-3

Mosbrugger, V., Utescher, T. & Dilcher, D.L., 2005. Cenozoic continental climatic evolution of Central Europe. Proceedings of the National Academy of Sciences, 102(42), 14964–14969. https://doi.org/10.1073/pnas.0505267102

Oaks, J.R., 2011. A time-calibrated species tree of Crocodylia reveals a recent radiation of the true crocodiles. Evolution, 65(11), 3285–3297. https://doi.org/10.1111/j.1558-5646.2011.01373.x

Pan, T., Miao, J.-S., Zhang, H.-B., Yan, P., Lee, P.-S., Jiang, X.-Y., Ouyang, J.-H., Deng, Y.-P., Zhang, B.-W. & Wu, X.-B., 2021. Near-complete phylogeny of extant Crocodylia (Reptilia) using mitogenome-based data. Zoological Journal of the Linnean Society, 191(4), 1075–1089. https://doi.org/10.1093/zoolinnean/zlaa074

Piras, P. & Buscalioni, A.D., 2006. *Diplocynodon muelleri* comb. nov., an Oligocene diplocynodontine alligatoroid from Catalonia (Ebro Basin, Lleida province, Spain). Journal of Vertebrate Paleontology, 26(3), 608–620. https://doi.org/10.1671/0272-4634(2006)26[608:DMCNAO]2.0.CO;2

Pomel, A.N., 1847. Note sur des animaux fossiles découverts dans le département de l'Allier. Bulletin de la Société géologique de France, 2e série, 4, 378–393.

Prangner, E., 1845. Über *Enneodon ungeri*, ein neues Genus fossiler Saurier aus den Tertiär-Gebilden zu Wies im Marburger Kreise Steiermark's. Steiermärkische Zeitschrift, Neue Folge, 8, 114–139.

Prista, G.A., Agostinho, R.J. & Cachão, M.A., 2015. Observing the past to better understand the future: a synthesis of the Neogene climate in Europe and its perspectives on present climate change. Open Geosciences, 7(1), 65–83. https://doi.org/10.1515/geo-2015-0007

Puértolas-Pascual, E., Blanco, A., Brochu, C.A. & Canudo, J.I., 2016. Review of the Late Cretaceous-early Paleogene crocodylomorphs of

Europe: Extinction patterns across the K-PG boundary. Cretaceous Research, 57, 565–590. https://doi.org/10.1016/j.cretres.2015.08.002

Rio, J.P. & Mannion, P.D., 2021. Phylogenetic analysis of a new morphological dataset elucidates the evolutionary history of Crocodylia and resolves the long-standing gharial problem. PeerJ, 9, e12094. https://doi.org/10.7717/peerj.12094

Rio, J.P., Mannion, P.D., Tschopp, E., Martin, J.E. & Delfino, M., 2020. Reappraisal of the morphology and phylogenetic relationships of the alligatoroid crocodylian *Diplocynodon hantoniensis* from the late Eocene of the United Kingdom. Zoological Journal of the Linnean Society, 188(2), 579–629. https://doi.org/10.1093/zoolinnean/zlz034

Roos, J., Aggarwal, R.K. & Janke, A., 2007. Extended mitogenomic phylogenetic analyses yield new insight into crocodylian evolution and their survival of the Cretaceous–Tertiary boundary. Molecular Phylogenetics and Evolution, 45, 663–673. https://doi.org/10.1016/j.ympev.2007.06.018

Ruebenstahl, A.A., Klein, M.D., Yi, H., Xu, X. & Clark, J.M., 2022. Anatomy and relationships of the early diverging Crocodylomorphs *Junggarsuchus sloani* and *Dibothrosuchus elaphros*. The Anatomical Record, 305(10), 2463–2556. https://doi.org/10.1002/ar.24949

Scheyer, T.M., Straehl, F.R. & Sánchez-Villagra, M.R., 2015. Crocodile in a Tree - An Exhibition on Evolution and Biodiversity. Scidinge Hall, Zurich, 87 p.

Serrano-Martínez, A., Knoll, F., Narváez, I. & Ortega, F., 2019. Brain and pneumatic cavities of the braincase of the basal alligatoroid *Diplocynodon tormis* (Eocene, Spain). Journal of Vertebrate Paleontology, 39(1), e1572612. https://doi.org/10.1080/02724634.2019.1572612

Skučas, P.P., Efimov, M.B. & Rezvyj, A.S., 2015. Nadotrjad Crocodyliformes. In Kurochkin, E.N., Lopatin, A.V. & Zelenkov, N.V. (eds), Fossil Reptiles and Birds. Part 3. In Vorobyeva, E.I., Kurochkin, E.N., Lopatin, A.V. & Shishkin, M.A. (eds), Fossil Vertebrates of Russia and Adjacent Countries: The reference book for paleontologists, biologists and geologists. GEOS, Moscow, 17–45. [In Russian].

Solé, F., Fischer, V., Denayer, J., Speijer, R.P., Fournier, M., Le Verger, K., Ladevèze, S., Folie, A. & Smith, T., 2021. The upper Eocene-Oligocene carnivorous mammals from the Quercy Phosphorites (France) housed in Belgian collections. Geologica Belgica, 24(1-2), 1–16. https://doi.org/10.20341/gb.2020.006

Springhorn, R., 1977. Revision der alttertiären europäischen Amphicyonidae (Carnivora, Mammalia). Palaeontographica A, 158, 26–113.

Teilhard de Chardin, P., 1915. Les carnassiers des phosphorites du Quercy. Annales de Paléontologie, 9, 103–191.

Turland, M., Larqué, P., Sudre, J., Vianey-Liaud, M. & Weber, F., 1993. Confirmation paléontologique du passage latéral des Calcaires de Ronzon aux Sables de la Laussonne dans le Stampien inférieur (Sannoisien) du bassin du Puy-en-Velay (Massif central). Géologie de la France, 1, 71–76.

Turner, A.H., Pritchard, A.C. & Matzke, N.J., 2017. Empirical and Bayesian approaches to fossil-only divergence times: A study across three reptile clades. PLoS ONE, 12(2), e0169885. https://doi.org/10.1371/journal.pone.0169885

Vaillant, L., 1872. Étude zoologique sur les crocodiliens fossiles tertiaires de Saint-Gérand-le-Puy. Annales des Sciences géologiques, 3, 1–58.

Van Baelen, A., Poot, N., Beirinckx, L., Bogaerts, A., Bellefroid, E., Claerhout, T., De Smedt, S., Dugardin, C., Engledow, H., Leliaert, F., Ossaer, J., Pereboom, Z., Semal, P., Slos, D., Smirnova, L., Vandepitte, L., Veltjen, E. & Trekels, M., 2022. DiSSCo-Flanders WP2 - task 2.1, Detailed inventory of the collections: Report. Instituut voor Natuur- en Bosonderzoek, Brussel, 31 p. https://doi.org/10.5281/zenodo.6511351

Venczel, M., 2023. Updating the fossil record of the alligatoroid crocodylian *Diplocynodon* from the late Eocene of Transylvanian Basin. Frontiers in Amphibian and Reptile Science, 1, 1217025. https://doi.org/10.3389/famrs.2023.1217025

Venczel, M. & Codrea, V. A., 2022. A new late Eocene alligatoroid crocodyliform from Transylvania. Comptes Rendus Palevol, 21(20), 411–429. https://doi.org/10.5852/cr-palevol2022v21a20

von Meyer, H., 1854. Mittheilungen an Professor Bronn gerichtet. Neues Jahrbuch für Mineralogie, Geognosie, Geologie und Petrefaktenkunde, 1854, 575–581.

Walter, J.D., 2025. Origin, diversity and evolution of the most common crocodylians of Europe in the Paleogene greenhouse context. Unpublished Ph.D. Thesis, Università di Torino, Torino, and Eberhard Karls Universität Tübingen, Tübingen, 452 p. https://hdl.handle.net/2318/2074751

Walter, J.D., Massonne, T., Paiva, A.L.S., Martin, J.E., Delfino, M. & Rabi, M., 2025. Expanded phylogeny elucidates *Deinosuchus* relationships, crocodylian osmoregulation and body-size evolution. Communications Biology, 8, 611. https://doi.org/10.1038/S42003-025-07653-4

Walter, J.D., Macaluso, L., Martin, J.E., Grohrock, T., Rabi, M. & Delfino, M., 2026. Taxonomic and quantitative reassessment of *Diplocynodon*, the most common crocodyliform in the Cenozoic of Europe. Palaeontology, 69(3), e70058. https://doi.org/10.1111/pala.70058

Wattinne, A., Vennin, E. & De Wever, P., 2003. Evolution of carbonated, lacustrine environment, with stromatolites: a paleoecological approach (quarry of Montaigu-le-Blin, Limagne graben, Allier, France). Bulletin de la Société géologique de France, 174(3), 243–260. https://doi.org/10.2113/174.3.243

Westerhold, T., Marwan, N., Drury, A.J., Liebrand, D., Agnini, C., Anagnostou, E., Barnet, J.S.K., Bohaty, S.M., De Vleeschouwer, D., Florindo, F., Frederichs, T., Hodell, D.A., Holbourn, A.E., Kroon, D., Lauretano, V., Littler, K., Lourens, L.J., Lyle, M., Pälike, H., Röhl, U., Tian, J., Wilkens, R.H., Wilson, P.A. & Zachos, J.C., 2020. An astronomically dated record of Earth's climate and its predictability over the last 66 million years. Science, 369(6509), 1383–1387. https://doi.org/10.1126/science.aba6853

Wood, S., 1846. On the discovery of an alligator and of several new Mammalia in the Hordwell Cliff; with observations upon the geological phenomena of that locality. The London Geological Journal, and Record of Discoveries in British and Foreign Paleontology 1, 1–7.